Motion feedback in the teleoperation of Unmanned Aerial Vehicles

Dissertation

der Mathematisch-Naturwissenschaftlichen Fakultät
der Eberhard Karls Universität Tübingen
zur Erlangung des Grades eines
Doktors der Naturwissenschaften
(Dr. rer. nat.)

vorgelegt von
Johannes Lächele
aus Singen

Tübingen
2017

Gedruckt mit Genehmigung der Mathematisch-Naturwissenschaftlichen Fakultät der
Eberhard Karls Universität Tübingen.

Tag der mündlichen Qualifikation:	20. Dezember 2017
Dekan:	Prof. Dr. Wolfgang Rosenstiel
1. Berichterstatter:	Prof. Dr. Heinrich H. Bülthoff
2. Berichterstatter:	Prof. Dr. Andreas Zell

Summary

Teleoperation of unmanned vehicles is a valuable tool in scenarios where the operator can not or should not operate the vehicle from on-board. Applications range from hazardous environments where exposure needs to be avoided, control of Unmanned Aerial Vehicles (UAV) to retrieve overviews of inaccessible disaster areas, to deep sea exploration where on-board operation is simply not possible.

However, limitations in sensor performance, noise and latencies introduced in the transmission, and ineffective display of the information to the operator can lead to a reduced amount of information, reduced performance, a loss of situation awareness, and in the worst case a loss of the remote vehicle. The spatial decoupling between the operator and the vehicle is one of the main challenges in teleoperation.

Most setups include one or more control sticks to steer the vehicle, a monitor displaying the live video feed of the main vehicle camera, and a seat for the operator. This can be extended by displaying additional state information using monitors or visual overlay, rendered on top of the main video stream [Tvaryanas, 2004; van Erp, 2000]. However, processing of multiple screens can increase mental workload. This can cause the operator to miss important information, leading to a loss of situation awareness and reduced performance or a crash of the vehicle.

Instead of presenting information purely visually, other feedback modalities can be used to convey vehicle state or information about the task. The goal of this PhD thesis is to investigate the possibility of providing additional information using motion feedback. Here, motion feedback is defined as physically moving the operator using a motion simulator. In the work presented in this thesis a distinction

between two motion feedback types is made. *Vehicle-state motion feedback* describes vehicle motion, while *task-related motion feedback* is the result of the combination of desired and actual vehicle motion.

To investigate the effects of motion feedback in teleoperation several studies have been conducted. In the experiments presented participants either controlled a virtual quadrotor flying in a simulated environment or a real octorotor. Participants controlled the UAV from within the CyberMotion Simulator (CMS), an 8-DOF motion simulator located at the Max Planck Institute for Biological Cybernetics.

The results show that providing motion feedback has a positive effect on performance in teleoperation of remote UAVs. If the remote vehicle is subject to external disturbances, e.g., wind gusts, vehicle-state feedback showed to improve disturbance rejection capabilities leading to increased performance. Furthermore, motion feedback can be shaped to include additional information about the task with positive effects on performance. This shows that the additional information included in the motion feedback can be used by the operator to improve performance and control behavior.

Zusammenfassung

Die Teleoperation eines unbemannten Gefährts ist ein wertvolles Werkzeug in Situationen, in denen der Pilot das Gefährt nicht von Bord aus steuern kann oder sollte. Beispiele hierfür reichen von, für den Piloten, toxischen Umgebungen, über Luftaufnahmen von Katastrophengebieten mithilfe von unbemannten Flugzeugen (engl. Unmanned Aerial Vehicle(UAV)), bis zur Erforschung der Tiefsee, bei der die Steuerung von Bord schlichtweg unmöglich wird.

Allerdings führen Einschränkungen in der Sensorerfassung, Rauschen und Latenzen in der Übertragung, sowie eine ineffiziente Darstellung der Informationen für den Piloten dann zu einem reduzierten Informationsfluss, reduzierter Leistung, einem Verlust des Situationsbewusstseins und im schlimmsten Fall zu einem Verlust des Gefährts. Die räumliche Entkopplung zwischen dem Piloten und des Flugobjekts ist eine der wichtigsten Herausforderungen in der Teleoperation von UAVs.

Die meisten Kontrollstationen beinhalten ein oder mehrere Steuerknüppel um das Gefährt zu steuern, einen Monitor der eine direkte Videoübertragung der Hauptkamera anzeigt und ein Sitzplatz für den Piloten. Dies kann erweitert werden, in dem zusätzliche Statusinformationen mit weiteren Monitoren oder visuellen Überlagerungen, die über die Hauptübertragung gezeichnet werden, angezeigt werden [Tvaryanas, 2004; van Erp, 2000]. Jedoch kann die Verarbeitung mehrerer Bildschirme die mentale Belastung erhöhen. Dies kann dazu führen, dass der Pilot wichtige Informationen nicht aufnimmt, was zu einem Verlust des Situationsbewusstseins und einhergehender reduzierten Leistung oder einem Unfall des Gefährts führt.

Anstatt Information rein visuell zu präsentieren, können andere Modalitäten genutzt werden Rückmeldungen über den Status des Gefährts oder Informationen über die Aufgabe zu präsentieren. Das Ziel dieser Doktorarbeit ist die Untersuchung der Modalität der Bewegung. Es soll untersucht werden, ob Bewegungen genutzt werden können, um dem Piloten zusätzliche Rückmeldungen über den Zustand des Gefährts bereit zu stellen. Bewegungsfeedback beschreibt hier die physikalische Bewegung des Piloten mit Hilfe eines Bewegungssimulators. In dieser Arbeit wird zwischen zwei Typen von Bewegungsfeedback unterschieden. *Fahrzeugzustandsbewegungsfeedback* beschreibt die Bewegung des Fahrzeugs, während *Aufgabenabhängiges Bewegungsfeedback* die Kombination aus tatsächlichem und gewünschtem Fahrzeugzustand ist.

Die Effekte von Bewegungsfeedback in der Teleoperation wurden in mehreren Studien untersucht. In den vorgestellten Experimenten kontrollierten Teilnehmer entweder einen virtuellen Quadrotor, der in einer simulierten Umgebung flog, oder einen echten Octorotor. Die Teilnehmer steuerten das UAV von der Kanzel des CyberMotion Simulators (CMS) aus, ein 8-DOF Bewegungssimulator, der sich am Max-Planck-Institut für biologische Kybernetik befindet.

Die Ergebnisse zeigen, dass die Bereitstellung von Bewegungsfeedback positive Effekte auf die Leistung und das Verhalten des Piloten in der Steuerung des UAVs hat. Ist das UAV externen Störungen ausgesetzt, wie z.B. Windstößen, zeigte sich, dass Fahrzeugzustandsbewegungsfeedback die Fähigkeit der Störungsunterdrückung des Piloten verbessert, was zu Leistungsteigerungen führt. Außerdem zeigte sich, dass Bewegungsfeedback dahingehend geformt werden kann, zusätzliche Informationen über die Aufgabe bereitzustellen. Dies zeigt, dass die zusätzlichen Informationen vom Piloten genutzt werden können um Leistung und Kontrollverhalten zu verbessern.

Acknowledgements

First, I want to thank my supervisors, Dr. Paolo Pretto and Dr. Joost Venrooij, for their patience, advice, and the occasional nudge in the correct direction during the time of this project. I am most grateful to my advisors Prof. Dr. Heinrich H. Bülthoff for giving me the opportunity and support to work on this project and Prof. Dr. Andreas Zell for the support on the part of the University of Tübingen.

I feel myself incredibly lucky to have met so many inspiring, intelligent, creative, and funny people during my time at the Max Planck Institute for Biological Cybernetics. I will always treasure the friendships formed during this time.

Words won't do justice for how grateful I am to have my wife Maria in my life, yet words are all I have. I could always count on her love, patience, and support during this journey.

Finally, I would like to thank my family for the love and support I have received throughout my life.

Contents

Chapter 1
Introduction

This introduction serves multiple purposes. First, definitions for teleoperation and a short overview of its history will be given. This is followed by the definition and an overview of Unmanned Aerial Vehicles (UAVs). In the third part motion feedback and its motivation is provided. These three research areas define the basis and the context of the work presented in this thesis. In the fourth and final part of this introduction the research questions will be presented and an outline for the following chapters will be given.

1.1 Teleoperation

1.1.1 Definition

The word *teleoperation* itself allows for an intuitive understanding of what it is. The greek prefix "tele-" translates to "far" or "from a distance" and "to operate" is to control the function of a machine or a system. Therefore, teleoperation describes all scenarios where a machine or system is being controlled (operated) from a distance.

However, this intuitive definition is too broad since it makes no assumption about the type of machine being controlled, the technology used to enable the control, and how the operator, i.e., the human controller, interacts with the machine. Can remotely switching channels on a television set already be considered teleoperation? Strictly following the intuitive definition, the answer should be yes. However, few would refer to switching channels as teleoperation, especially since the device used for doing so is called remote control.

The Oxford Dictionary defines *remote-control* as the "control of a machine or apparatus from a distance by means of radio or

infrared signals transmitted from a device". A perfect description of the television example and a good description of the intuitive understanding of teleoperation.

But there is more to teleoperation than the remote control of a machine or vehicle. In order to move from a remote-control scenario to teleoperation the unidirectional communication from the operator to the vehicle has to be changed to a bidirectional channel. Furthermore, the terms used in literature are not consistent. For example, in [Cui et al., 2003] *teleoperation* is defined only in the context of controlling a remote robotic arm, which excludes many other types of devices, like mobile robots or industrial plants.

A better approach was taken by Sheridan, who included the relationship to human perception and action in the definition: "Teleoperation is the extension of a person's sensing and manipulation capability to a remote location" [Sheridan, 1989]. This definition makes no assumptions about the device being controlled and the technologies used to implement them. However, the inclusion of sensing capabilities in the definition sets teleoperation apart from remote-control. This definition implies that the communication channel from the operator to the remote vehicle is extended to include communication from the vehicle to the operator. Teleoperation is therefore an extension of remote control with an additional communication channel.

This definition allowed Sheridan to further extend it to *telerobotics* and *telepresence*. Telerobotics is the supervision of an autonomous remote robot by a human operator. Telepresence "is the ideal of sensing sufficient information about the teleoperator and task environment, and communicating this to the human operator in a sufficiently natural way, that the operator feels physically present at the remote site" [Sheridan, 1989]. Furthermore, Sheridan's definition of teleoperation includes devices such as robotic arms that are fixed on a stationary platform. This definition is less strict to what is found in other work, e.g. [Cui et al., 2003], where this would be the only teleoperation scenario.

Sheridan's definition of teleoperation describes the control scenarios presented in this thesis very well. However, the scenarios always describe a single operator controlling a remote vehicle (e.g., a

simulated quadrotor or octorotor), which is only a small subset of all possible teleoperation scenarios. This does not cause any violations of the definition and also does not break the possible applicability of motion feedback in other teleoperation scenarios. In this work we will refer to teleoperation as the remote control of UAVs following Sheridan's definition.

1.1.2 History

The foundation of teleoperation is the remote-control of devices or machines. The idea of remotely controlling a vehicle has been around for a long time. In November, 1898 Tesla patented an apparatus that allowed the remote control of a small boat [Tesla, 1898]. The boat could be controlled without the need of a wired connection, i.e. a tethering cable, and can be seen as the first ever remote-controlled vehicle. This was shortly followed by the Telekino [Pérez Yuste, 2008] presented at the Centre for Aeronautical Tests formed by the Spanish Government in January 1904. The device consisted of a tricycle that could be wirelessly controlled from a distance of up to 30 m using a wireless telegraph system that would transmit Morse code. Due to advances in radio guidance systems during World War I and World War II, the first fully-functional remote-controlled model airplane was released in 1939: the "Big Guff", constructed by Walter and William Good.

Visual feedback, i.e., presenting live view from a camera mounted on the remote vehicle, is arguably the most important information that needs to be transmitted from the vehicle to the operator. The difficulty is that visual information can easily take up a lot of capacity of the communication channel. The capacity needed to transmit video information is dependent on the multiplicative of frame rate, horizontal and vertical resolution, color information, and sample resolution. As an example, transmitting uncompressed grayscale video with a resolution of $640\,\mathrm{px} \times 480\,\mathrm{px}$, a frame rate of 30 Hz, and a sample resolution of 8 bit requires a bandwidth of $640 \cdot 480 \cdot 30 \cdot 8 = 73\,728\,000\,\mathrm{bit\,s^{-1}}$ or $8.78\,\mathrm{MB\,s^{-1}}$. However, at the time when remote-control became available to the masses (1940's

and 1950's), the technology needed for such a setup was only available in science-fiction [Heinlein, 1942].

From the first successful remote-control to first teleoperation setups almost 90 years passed until the technology emerged that allowed using wireless transmission of a video signal. In the late 1970's and early 1980's the first results of teleoperation experiments were presented. The experiments highlighted the difficulties of providing visual feedback [Bejczy, 1980; Brye et al., 1977; Cole and Kishimoto, 1980; Crooks et al., 1975; Ranadive, 1980].

Providing satisfactory visual feedback is still challenging, even after roughly 40 years of research between the first setups and today. The main problem is that the technical aspects of the setup and how they are implemented greatly affect operator performance. In their review [Chen et al., 2007], Chen et al. show how the effects of field-of-view, camera orientation, number of cameras, frame rate, and time delays affect operator performance.

Although challenges remain, teleoperation of remote vehicles is an established concept that is used in research, industrial, and recreational areas. The advances in technology allow for building smaller devices, e.g., sensors (cameras), actuators, batteries, with increased capabilities, e.g., wide range of sensing, dexterous control, small size and weight, longer lifetime. This extends the possible application of teleoperated vehicles, which will be discussed in the next section.

1.1.3 Application

Many scenarios exist where access to a location or environment involves taking large risks or is simply impossible for humans. Handling hazardous materials, like radiating, toxic, or infective goods, requires stringent safety precautions and protective gear that shields the handler from any exposure. But the equipment used has limits, e.g., gamma radiation penetrates the suits tissue almost unhindered, effectively rendering the suit's protection useless.

Some environments are simply not accessible for humans. Consider a team of marine biologists exploring the deep sea. Although, many manned underwater research vessels can easily reach depths

of several hundred meters, the development of vessels that can go deeper becomes significantly more challenging. In addition, the benefits of using a Remotely Operated Underwater Vehicle (ROV) outweigh the use of a manned vehicles. ROVs are small underwater vessels equipped with an array of sensors, e.g., cameras, lights, and actuators that allow for agile control. A zero buoyancy cable connected to a research boat supplies it with power and establishes communication. The most important benefit, however, is that the controlling human is never at risk, only the hardware is lost in case of an accident. In addition, time-costly exchanges of on-board control teams of manned vehicles can be saved. It is even possible to continuously operate the ROV, with multiple teams sharing the work of controlling the ROV.

Another example is the use of an Unmanned Aerial Vehicle (UAV) to perform visual inspections of wind turbines. The blades of a wind turbine are mounted in heights of around 50–150 m. Reaching the top of these structures is time-consuming for a technical inspection team. Furthermore, a team working in these heights is required to closely follow safety procedures to avoid accidents. In contrast a UAV can reach these heights faster, while avoiding to expose an inspection team to any risks. Even the tips of the blades, due to their flexible design unreachable for a human inspector, can be inspected closely. Using live video feedback and video recording equipment, the inspection process can be completed from a safe location. Furthermore, recorded video allows for a simultaneous analysis by multiple experts and can be archived for later use, e.g., verification purposes.

Teleoperation of remote vehicles introduces a wide range of possible applications in many different areas. Although technical challenges persist, the concept has matured to a state that it can be routinely used in many applications.

1.2 Unmanned Aerial Vehicles (UAVs)

Teleoperation of vehicles includes challenges that do not exist in other teleoperation setups. All equipment required to complete the

task needs to be carried along with the teleoperated vehicle. To ensure the dexterity of the setup, i.e., no movement restrictions, the equipment has to be powered and carried by the vehicle itself. This reduces operation time of the vehicle since additional power is required and payload is increased.

Furthermore, to allow for the information of on-board sensors to reach the operator, a tethered connection severely limits vehicle movements calling for wireless bidirectional transmission systems. Due to their design, wireless communication is prone to interference with other transmission systems. To ensure reliable communication additional en-/decoding steps are required that reduce channel capacity.

Airborne vehicles are especially affected by these challenges. Maintaining stable flight velocity or position requires the vehicle to constantly consume power. This is different to ground vehicles where the vehicle remains stable with its drive mechanisms switched off. For aerial vehicles, power consumption increases significantly with increased payload, which can reduce operation time significantly.

Although UAVs are usually more complex in their construction and control than their ground counterparts, the ability to easily get broad overview imagery, inspect details in otherwise unaccessible areas, and fast traveling speeds are considerable advantages over ground vehicles. Those features make UAVs predestined for inspection, search and rescue, and exploration tasks. Especially UAVs capable of vertical take-off and landing (VTOL) with the ability to hover at a fixed location find their application as a "flying eye in the sky" for tasks that require the operator to operate visually in a remote environment. For these reasons, when referred to teleoperation in this thesis, the teleoperation of a remote UAV will be assumed.

The work presented in this thesis shows teleoperation scenarios where a remote quadrotor is being controlled in different teleoperation tasks. Quadrotors belong to the class of multirotors, i.e., UAVs with VTOL capabilities. Multirotors have many advantages over other VTOL UAVs, like a redundant propulsion system, a less

complicated control paradigm – especially in comparison with helicopters – and relative to their own size and weight, multirotors have a large payload. The work of [Bouabdallah et al., 2004] and [Hua et al., 2009] provide an excellent overview over the design and control of quadrotors.

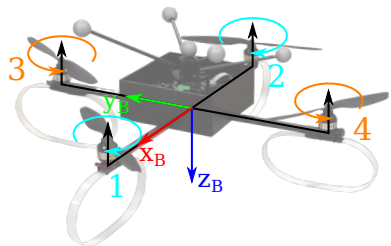

(a) Quadrotor frame with reference frames and motor spin direction.

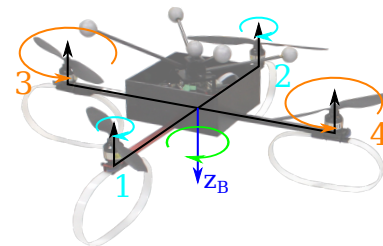

(b) Motor spin velocity is reduced for 1 & 2 and increased for 3 & 4, resulting in a yaw rotation around Z_B.

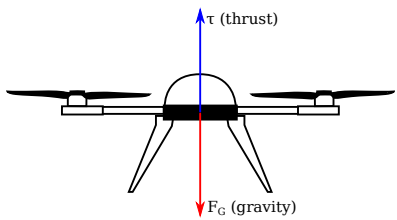

(c) Stable hover, all motors spin velocities are equal. Thrust compensates effects of gravity, $\tau = -F_G$.

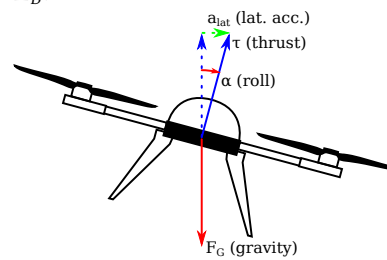

(d) Motor 3 spins faster than motor 4 resulting in a roll motion α and an acceleration in direction of roll a_{lat}.

Figure 1.1: Schematic overview of control of quadrotor motion.

Quadrotors have four propellers that are arranged in pairs at the opposite side of the frame, see fig. 1.1a. Each pair of propellers spins in the same direction resulting in the moments adding up with the point of actuation in the center of the frame. The second pair of propellers is arranged in the same way, but rotated by 90° to the previous pair of propellers. The direction of spin is in the opposite

direction than the direction of the first pair. In the stable hover condition (fig. 1.1c), all propellers spin with the same speed, resulting in two moments of the same magnitude but opposite directions acting on the frame. These moments cancel each other out and as a result only a thrust force is acting on the frame and pointing downwards. Thereby, compensating the effects of gravity; the quadrotor is in hover. Fig. 1.1c shows how the thrust *tau* generated by the motors compensates the effects of gravity F_G.

Lateral and longitudinal motion is controlled by changing the rotational speed of the propellers. Lateral motion is achieved by reducing the speed of one of the propellers while increasing the speed of the propeller on the opposite side. This results in a moment acting on the frame around the roll axis causing it to rotate. As a result the thrust vector changes its direction, which can be expressed by a split into a vertical component and a horizontal component. Fig. 1.1d shows how the frame is rotated, causing the thrust vector τ to change direction. The horizontal component a_{lat} accelerates the quadrotor in the direction of rotation. Since the overall thrust did not change in magnitude the vertical component is reduced and not large enough to fully compensate effects of gravity. This results in a loss of altitude, which needs to be compensated by increasing the rotational speeds of all propellers. Due to the similarities in the design of the quadrotor, longitudinal motion is implemented analogously.

To change the heading of the frame, the speeds of one pair of propellers is reduced and the speeds of the other pair increased in such a way that the thrust remains constant. However, due to the non-zero difference in moments, the heading angle of the frame is changing, see fig. 1.1b.

Quadrotors are controlled by defining desired roll and pitch angles, heading rate of change and thrust. An on-board controller takes the desired state as input and changes the speeds of the propellers accordingly to reach the desired state. With the help of an on-board Inertial Measuremnt Unit (IMU) that measures attitude and angular velocities, PID controllers for the roll and pitch angles can be implemented. The heading rate of change can be implemented with a PD controller. The desired thrust input controls the rotational speeds

of all propellers simultaneously. For a human operator controlling a quadrotor is easier compared to controlling a helicopter, because the controllable states are decoupled. This means that a roll input does not influence the heading of the quadrotor as it is the case for a helicopter.

However, it is important to note that moving a quadrotor is a combination of rotation followed by a linear acceleration. In a stable hover position, quadrotors are horizontal, assuming there are no disturbances that need to be compensated by moving the quadrotor. Since quadrotors move by changing the orientation of the thrust vector, the frame is rotated. This is important to consider in applications where it is important to keep a constant orientation of the frame. Consider the case where a quadrotor is used for visual examination of a power plant. Due to wind disturbances corrective inputs have to constantly be provided so that the quadrotor can keep its location. With a camera fixed to the frame of the quadrotor the resulting inspection video will contain a lot of movements resulting in barely, if not entirely unusable material. A solution to this problem is the use of an additional camera stabilization system, i.e., an actuated gimbal. The gimbal is able to compensate the movements of the quadrotor frame automatically, resulting in an undisturbed video. In the experiments presented as part of this thesis, it is assumed that the video camera is mounted on a gimbal system capable of compensating roll, pitch, and yaw rotations.

1.3 Motion feedback

One of the major challenges in teleoperation is that the operator is faced with a reduced amount of information to control the vehicle. All information needed by the operator to control the system needs to be sensed on-board and sent to the operator. There the information needs to be presented to the operator in a meaningful way. This is in clear contrast to direct control of vehicles, where the operator is on-board the vehicle. The senses of the operator can either directly perceive the information needed for controlling the

vehicle or sensors provide information that can be displayed to the operator, eliminating the need for a troublesome transmission.

Controlling a vehicle requires the operator to see where the vehicle is going in order to navigate safely through the environment. A live video feedback is therefore crucial for a teleoperation scenario where the operator directly controls the vehicle. With increased autonomy this visual feedback usually changes to a top-down view where the position of the vehicle is indicated on top of a map. Providing effective visual feedback is a research topic in itself, Chen et al. [Chen et al., 2007], Cole and Kishimoto [Cole and Kishimoto, 1980], and Crooks et al. [Crooks et al., 1975] provide an excellent overview of the issues involved.

With the operator not being able to perceive the state of the vehicle directly, additional feedback is necessary. This information is important for the operator to avoid the vehicle reaching a state where it can not be recovered from. Usually, the ground control station is equipped with additional displays that show the state of the vehicle, e.g., orientation, velocity, engine temperature.

However, monitoring multiple displays can put a lot of mental effort on the operator. The attention of the operator is split across the displays, which can lead to the operator missing crucial information since too much time is put on other displays [Tvaryanas, 2004]. This increases the chance of a loss of situation awareness, leading to accidents and in the worst case a loss of the remote vehicle. Note, that this problem also exists in the on-board control of vehicles, e.g., controlled flight into terrain (CFIT) [Breen, 1999].

Another approach involves the use of displays that provide non-visual feedback about the state of the vehicle. There are examples where auditory, vibro-tactile, or haptic displays were successfully used in the control of vehicles. Some displays provide additional auditory cues to inform the operator of the state of the vehicle or the task in the remote environment [Apostolos et al., 1992; Lokki and Gröhn, 2005]. Vibro-tactile displays have been used successfully to alert the operator of incoming disturbances in a landing task [Steele and Gillespie, 2001]. By actuating the control stick, haptic cues can be displayed to the operator, with successful application in collision

avoidance [Lam et al., 2007] or trajectory following [Alaimo et al., 2010] tasks.

The performance of humans to visually detect accelerations is very poor [Monen and Brenner, 1994] compared to the vestibular system. The vestibular system is part of the inner ears and perceives angular velocities and accelerations. In comparison to vision, the vestibular system is faster in detecting accelerations. Controlling a vehicle requires the operator to know how it is moving in space. By providing vehicle-related motion feedback, i.e., moving the operator according to the movements of the vehicle, the operator is able to faster detect changes in the movements of the vehicle leading to increased control performance [Ricard and Parrish, 1984; Zaal et al., 2009].

Providing motion feedback to the operator is a common practice in vehicle simulation for several decades. The goal of vehicle simulation is to create a controlled environment where humans behavior can be studied. This includes training in operating vehicles, solving complex tasks, and decision making in stressful situations.

To recreate the sensation of controlling a vehicle as realistic as possible, some setups provide motion feedback where the perceived motion matches the actual vehicle motion as close as possible. This is important, since it improves the sense of presence of the operator. It also ensures the applibility of findings to real world scenarios and avoids negative transfer of training.

In cases where the operator knows the vehicle, an expectation of how the perceived motion in the simulator should feel is formed. Providing motion feedback that does not comply with the expected motion can result in the motion feedback to be a disturbance to the operators performance. In addition, these unexpected motion cues may lead to motion sickness, further impacting operator performance and a reason to stop further experiments [Oman, 1990].

The experiments conducted by Ricard and Parrish [Ricard and Parrish, 1984] show that providing motion feedback in a helicopter control task significantly increases operating performance. The work of Scanlon [Scanlon, 1987] also showed a significant performance increase in conditions that included motion feedback. However, this was only found in the most complex approach tasks defined for the

experiment. This is also the conclusion made in the work of [Hall, 1989], where motion feedback becomes increasingly important as the tasks becomes more demanding. Given the challenges seen in teleoperation, e.g., time delays or low quality feedback, it is reasonable to assume that providing additional motion feedback in a teleoperation scenario has positive effects on operator performance or behavior.

The results of [Robuffo Giordano et al., 2010] show that providing motion feedback in a teleoperation precision hover task changes operator behavior. Participants showed a more "gentle" control behavior where the amount of control inputs was reduced in motion feedback conditions. This was explained with a phenomenon denoted as "shared fate" [Hing and Oh, 2009]. The increased situation awareness leading to less strong inputs given by the operator to avoid strong motion feedback. This in turn reduced the possibility of putting the frame of the remote vehicle under too much structural stress.

In teleoperation setups there is a spatial decoupling between the operator and the controlled vehicle. This grants a certain freedom in how the motion perceived by the operator can be defined. The idea that motion feedback can be shaped in order to improve operator performance is the core idea of this thesis.

1.4 Thesis outline

In the first chapter of this thesis the effectiveness of providing vehicle-related motion feedback, i.e., moving the operator in a similar way as the vehicle is moving, is investigated. Based on the positive results of previous research in teleoperation [Robuffo Giordano et al., 2010] and vehicle simulation [Ricard and Parrish, 1984; Scanlon, 1987; Zaal et al., 2009] a performance increase in a precision hover task can be expected.

Although teleoperation of UAVs shares similarities to on-board operation, the spatial decoupling defines the key difference between teleoperation and vehicle simulation. We hypothesize that this introduces the freedom to shape the motion feedback presented to

the operator. The second chapter of this thesis investigates whether different components of the motion feedback affect performance differently. In addition, we test the effectiveness of task-related motion feedback, which includes information beneficial to the task at hand. For this we defined a desired target state, calculated the difference to the actual vehicle state and presented this offset as a roll motion. The resulting motion does not describe vehicle motion but instead it provides performance feedback in completing the task.

In the experiments presented in the first two chapters participants controlled a simulated quadrotor in a simulated environment. This approach guarantees a controlled experimental environment where external influences are reduced to a minimum. It does not, however, show whether motion feedback in teleoperation is a feasible approach in real teleoperation setups. This issue is addressed in the third chapter of this thesis that acted as a reproduction of a previous experiment, where the controlled vehicle was being simulated. In this experiment participants controlled a real vehicle, i.e., an octorotor, while experiencing different types of motion feedback that follow the same definition as in the previous experiment.

In the final experiment presented in the fourth chapter we address two questions. Does task-related motion feedback improve performance in tasks other than precision hovering? How do the improvements of providing motion feedback compare to a commonly used approach in teleoperation, i.e. haptic feedback?

Chapter 2

Motion feedback improves performance in teleoperating UAVs

2.1 Can motion feedback improve teleoperation performance?

Teleoperation, i.e., the operation of a vehicle from a distance, is known to be difficult. The challenge partly arises because the vehicle state needs to be sensed on-board, transmitted to the operator's location, and represented to the operator in an informative way. This process may introduce noise and delays, reducing operator's situational awareness and compromising the ability to control the vehicle.

Traditional teleoperation setups use a stationary ground control station to provide the operator mainly with visual and haptic information retrieved from the vehicle [Chen et al., 2007]. However, in unknown and unstructured environments, visual and/or haptic information alone may not be sufficient to timely detect sudden changes in the vehicle state. The lack of information could then result in poor performance or even lead to dangerous situations, e.g., wind gusts while hovering an unmanned aerial vehicle (UAV) might result in loss of control.

A possible way to improve teleoperation performance is to provide more information to the operator by introducing feedback about the actual motion of the controlled vehicle. In vehicle simulation research it has already been shown that motion feedback has a beneficial effect on pilot training for controlling aircraft and

rotorcraft [Ricard and Parrish, 1984; Scanlon, 1987]. In flight simulation motion feedback is used to increase the realism of the pilot experience and to ensure a positive transfer of training to the real vehicle. However, teleoperated vehicles are not operated from aboard. Therefore, motion feedback for teleoperation does not necessarily focus on realistically representing the actual vehicle motion, but instead can represent informative, task-related characteristics of the vehicle state. In teleoperation there is therefore additional liberty in how motion feedback can be designed in order to enhance the operator's situational awareness and performance.

In our work we investigated whether adding motion information to visual feedback about a teleoperated UAV improves control performance. The motion of the remote vehicle was scaled and used as feedback for the operator in a motion simulator. This approach has some similarity to previous research found in [Hing and Oh, 2009; Ortiz et al., 2008; Robuffo Giordano et al., 2010]. However, in contrast to their work we provided motion feedback as the scaled motion of the remote vehicle. This way false cues introduced by the motion drive algorithm (MDA), e.g., rotations from tilt coordination and washout filters, are not introduced in this approach.

In addition, we made a first attempt to understand whether applying different scaling factors for vertical and lateral motion affects performance. We tested these hypotheses with a human-in-the-loop experiment in which participants were asked to control a simulated quadrotor and perform precision hovering in front of several targets in a virtual room.

The work described in this chapter has been published in:

Lächele, J., Pretto, P., Venrooij, J., and Bülthoff, H., "Motion feedback improves performance in teleoperating UAVs," *AHS International 70th Annual Forum*, May 2014.

2.2 The CyberMotion Simulator

The experimental setup consisted of 3 parts: The CyberMotion Simulator, the simulation of the remote environment with the remote vehicle, and the experimental control software, as depicted in Fig. 2.1.

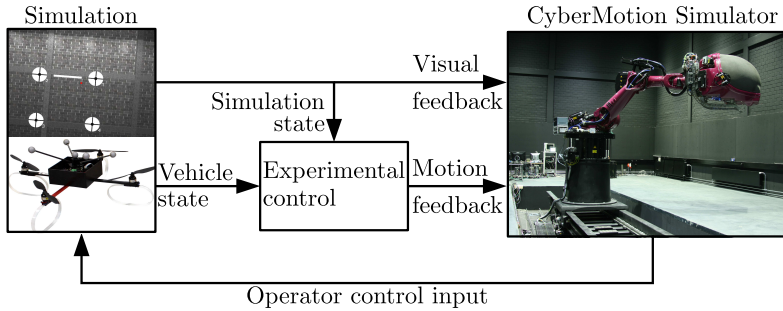

Figure 2.1: Overview of the Experimental setup showing the connection between the individual components.

The connections between the blocks in Fig. 2.1 show the flow of information.

The experiment was performed on the CyberMotion Simulator (CMS). The simulator consists of a standard 6 Degrees of Freedom (DOF) anthropomorphic robotic arm with a carbon fiber cabin attached as end-effector. The cabin is mounted on an actuated rail, therefore increasing the dexterity of the setup.

With its recently added linear axis the workspace of the simulator was further extended. Now, a wide range of lateral movements can be achieved in addition to the already high dexterity of the robot arm (see Fig. 2.2a). A detailed description on the mechanical setup and control of the CMS can be found in [Masone et al., 2011; Nieuwenhuizen and Bülthoff, 2013].

The motion of the CMS is controlled by a control algorithm that takes the position and velocity of the end-effector as input. This input is defined by the scaled state of the simulated quadrotor moving in the virtual environment. With a Jacobian inverse based approach the control algorithm then controls the CMS joints in order to track the input trajectory in Cartesian space. The design and implementation of this control algorithm can be found in [Masone et al., 2011]. Special care has been taken in the design of the experiment that all motion is within the movement envelope of the CMS.

Participants are seated inside of a closed cabin attached as the CMS end-effector. The cabin excludes unwanted external influences like noise, wind, and visual feedback. The inside of the cabin entry door serves as a projection screen for two projectors. The screen has a maximum vertical field-of-view (FOV) of 70° and a maximum horizontal FOV 140°. Fig. 2.2b shows the inside of the cabin with the seat for the participants, the cyclic control stick and the collective lever in front and on the left side of the seat, and the projectors in the upper right and left corners.

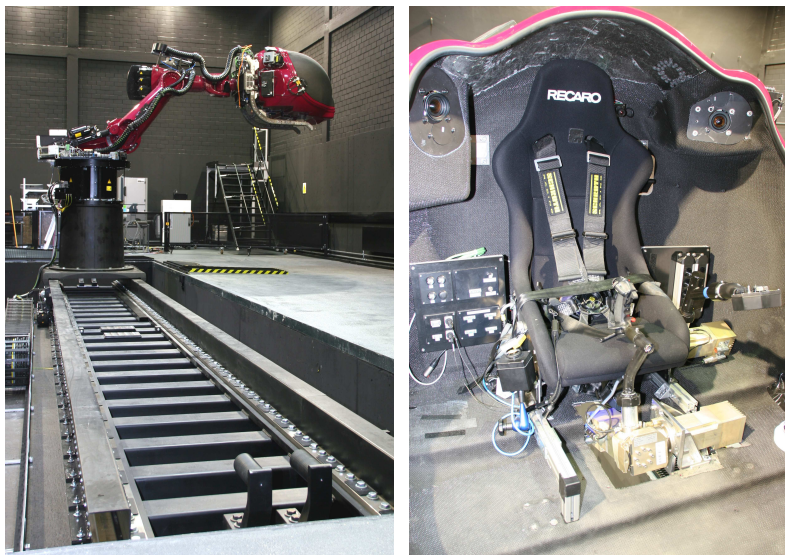

(a) CMS with closed cabin mounted on linear axis.

(b) Inside view of cabin with controls.

Figure 2.2: The CyberMotion Simulator (CMS) mounted on linear axis and inside view of cabin

2.3 Virtual environment

The virtual environment was modeled after the *TrackingLab*, a hall located at the Max Planck Institute for Biological Cybernetics using the game development engine *Unity3D*. The hall consists of a large free space of 12.8 m × 11.7 m × 5 m (width × length × height) and is used for tracking the position and orientation of marked objects. We decided to use this room as the remote environment since the tracking system can be used for later experiments with a real quadrotor flying in that room. Since the remote environments then look very similar, the results from future experiments in reality can then be compared.

The simulation consisted of two parts, the visual and the physical simulation. In the physical simulation the movements of the remote vehicle were calculated and the state of the vehicle was used to update the visual simulation. The visual simulation rendered the scene from the on-board camera and displayed the images on the curved screen inside the cabin of the CMS. This was done to be able to synchronize the motion of the CMS with the visual motion of the video stream.

As remote vehicle we used a simulated quadrotor, modeled after the behavior of a real quadrotor. Quadrotors are capable of vertical take-off and landing (VTOL) with the possibility of hovering and sideways motion. The real quadrotor is equipped with 3D-gyroscopes and 3D-accelerometers that enable the control of the roll and pitch orientation as well as yaw rate and thrust. The quadrotor is controlled by defining the desired roll ϕ, pitch θ, yaw rate $\dot{\psi}$, and thrust τ. An on-board control loop achieves the desired state by actuating the four propellers in such a way so that the resulting torques rotate the quadrotor to achieve the commanded state. Depending on the orientation and the amount of thrust, the quadrotor starts accelerating towards the tilted direction.

In the case of the simulated quadrotor a simplification has been made by assuming that three torques along the main axes and a vertical force defined in body frame can directly be applied to the rigid body. This is a valid simplification since in the case of the real quadrotor these torques and forces would be a direct result of the

control algorithm actuating the propellers. Details on the modeling and control of quadrotors can be found in [Bouabdallah et al., 2004]. A virtual camera was attached to the body frame of the quadrotor.

2.4 Disturbance signal

During all trials we simulated lateral wind gusts that disturbed the quadrotor; thereby, forcing participants to constantly correct the position of the vehicle. The wind disturbances acted on the vehicle only in the lateral direction and the applied forces were calculated using the following equation.

$$F_D(t) = \frac{1}{2}\rho C_D A \cdot (V(t) - \dot{y})^2 \tag{2.1}$$

The reference area $A = 0.25\,\mathrm{m}^2$, the drag coefficient $C_D = 1.05$ of the vehicle and the mass density $\rho = 1.2\,\mathrm{kg\,m}^{-3}$ of the surrounding air were assumed to be constant throughout the experiment. An in-depth derivation of (eq. 2.1) can be found in [Ruijgrok, 1996].

The wind velocity signal $V(t)$ at time t was defined as a multisine signal consisting of 10 frequencies (f_i) with 10 phase shifts (φ_i). See (Table 2.1) for the values used in this experiment.

$$V(t) = \sum_{i=1}^{10} \sin\left((2\pi f_i t) + \varphi_i\right) \tag{2.2}$$

2.5 Control inputs

Participants were controlling the vehicle using a control loading system (CLS), namely a collective control stick mounted on the left and a cyclic control stick mounted in front of the participants (see Fig. 2.2b). Both control devices are manufactured and distributed by *Wittenstein AG*. The stiffness of the cyclic stick was $33.18\,\mathrm{N/rad}$ over the full deflection range and its moment of inertia $0.4\,\mathrm{Ns}^2/\mathrm{rad}$; the damping coefficient was 2.18. The pitch axis of the cyclic stick was locked. The stiffness of the collective lever was $20.90\,\mathrm{N/rad}$ over the

Table 2.1: Frequencies and phase shifts used for multisine disturbance signal

Index i	Frequency f_i [Hz]	Phase φ_i [rad]
1	0.0300	2.5031
2	0.1378	1.4353
3	0.2456	-0.5854
4	0.3533	2.754
5	0.4611	-1.5367
6	0.5689	0.2084
7	0.6767	2.8573
8	0.7844	-1.4593
9	0.8922	-1.5703
10	1.0000	2.6871

full deflection range, the damping coefficient 3.65, and the moment of inertia 1.4 Ns^2/rad. In addition the friction force was set to 0.68 N

Inputs of the cyclic stick are denoted with α, while collective lever inputs are denoted with β. The deflection of the collective defines the amount of thrust given by the propellers of the quadrotor. The thrust vector is defined in body frame of the quadrotor and is always acting along $-p_{q,V}$. Please find an overview of the reference frames in Fig. 2.4. The position of the cyclic stick defines the desired roll angle of the quadrotor. The desired roll angle and thrust values are sent to the simulated quadrotor where an on-board control algorithm applies torques and forces on the quadrotor body in order to achieve the desired orientation and thrust.

2.6 Experiment description

In this experiment, participants were asked to complete a series of hover tasks while experiencing different types of motion feedback. At the beginning of each trial the vehicle was located on the floor of a virtual room. Participants then had to fly to the first target indicated by a number in the lower right corner of the target (see

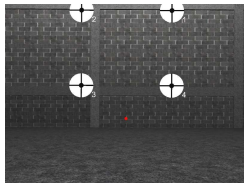

(a) At beginning of trial participants are placed on the ground

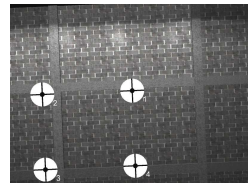

(b) Hover task started, the red visual reference has been removed

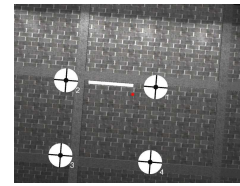

(c) Hover task complete, line shows direction to next target

Figure 2.3: Screenshots of the virtual environment with four targets attached to the wall, as seen from participants.

Fig. 2.3a). The targets as well as the order numbers were visible at all times during the trial.

The hover task started when participants were within the black center part of the target (see Fig. 2.3b). A series of beeps with gradually increasing pitch provided feedback about the duration of the hover task. All participants were carefully instructed to hover as precisely as possible in front of the center of a target. The hover task was complete after a period of 10 s and participants could proceed to the next target.

After completing a hover trial a white line appeared, showing the direction to the next target (see Fig. 2.3c). Before and after hover tasks a red dot was visible in the scene that represented the mapped position $\hat{p}_q$ of the quadrotor. This allowed participants to better orient themselves before the next hover task or for landing the quadrotor.

During the experiment participants were facing the same wall in front of them with the targets attached. Participants were only able to control the quadrotor in the vertical and lateral direction by using the collective lever and the cyclic stick. Movements of the quadrotor in the longitudinal direction, pitch rotations, and yaw rotations were locked. These restrictions were made for two reasons. First, this simplified the quadrotor control task, hence reducing the training time needed. Second, this prevented the quadrotor from moving in

the longitudinal direction, therefore keeping the distance to the wall and targets size on screen constant.

We created five conditions in which the motion feedback scaling with respect to the actual vehicle motion was systematically varied. The conditions are noted as follows: (a, b), where the lateral scaling gain a can vary between 0.0 and 0.4 and the vertical gain b between 0.0 and 0.2. In condition $(0.0, 0.0)$ no motion feedback was provided; in conditions $(0.1, 0.1)$ and $(0.2, 0.2)$ the motion scaling factor was 0.1 and 0.2 for both lateral and vertical motion respectively; in conditions $(0.2, 0.1)$ and $(0.4, 0.2)$ the lateral motion scaling was twice as much as the vertical motion scaling. Note that the scaling for lateral motion applied to the linear motion and the roll rotation, while the vertical scaling applied to the vertical motion only. This scaling applied to the physical motion only and was not applied to the visual motion of the virtual camera attached to the quadrotor.

The experiment was split into four sessions of 15 trials each. For each trial a participant completed four hover tasks, with the order of the targets randomized. For the analysis we only used the data of the last two sessions. In each session, each of the 5 conditions was repeated 6 times in a randomized order.

We considered the first two sessions as training with the first session having the same order of conditions for all participants. The first 6 trials of the first training session consisted of the no-motion condition and were followed by the remaining motion feedback conditions with gradually increasing motion feedback gain. This was done in order to allow participants to understand the task and the control of the quadrotor first, before introducing motion feedback.

During each of the hover tasks we measured the error, i.e., the distance of the quadrotor to the current target center. We use the accumulated error over the duration of the hover task as performance measure (eq. 2.3).

$$\mathrm{Err}_D = \int \|p_t - \hat{p}_q\| \, \mathrm{d}t \tag{2.3}$$

In addition we calculated the horizontal component (eq. 2.4) of the error, and the accumulated error of the vertical component (eq. 2.5) separately.

$$\mathrm{Err}_H = \int |p_{t,H} - \hat{p}_{q,H}| \, \mathrm{d}t \tag{2.4}$$

$$\mathrm{Err}_V = \int |p_{t,V} - \hat{p}_{q,V}| \, \mathrm{d}t \tag{2.5}$$

With p_t defined as the position of the current target in world frame. The vertical and horizontal components of the target position are denoted with $p_{t,V}$ and $p_{t,H}$. The orthogonal projection of the quadrotor position onto the plane where the targets reside is denoted with $\hat{p}_q$. The vertical and horizontal components of the projected position $\hat{p}_q$ are denoted with $\hat{p}_{q,V}$ and $\hat{p}_{q,H}$. The reference frames in Fig. 2.4 show where the individual frames are located in the virtual environment.

In addition, we recorded the inputs given by the participants during the hover task. For the analysis we calculated the root mean square (RMS) of the stick deflection to compare the effects of motion feedback scaling on the inputs given by the operator. We calculated the RMS for both control sticks (eq. 2.6),

$$\mathrm{RMS}_c = \sqrt{\sum_{i=1}^{n} \frac{1}{n} (\alpha_i^2 + \beta_i^2)} \tag{2.6}$$

the cyclic stick (eq. 2.7), and the collective lever (eq. 2.8).

$$\mathrm{RMS}_\alpha = \sqrt{\sum_{i=1}^{n} \frac{1}{n} \alpha_i^2} \tag{2.7}$$

$$\mathrm{RMS}_\beta = \sqrt{\sum_{i=1}^{n} \frac{1}{n} \beta_i^2} \tag{2.8}$$

Due to the incorporation of squared values into the measure, the RMS suppresses smaller values, while at the same time reinforcing the influence of large control inputs in the final result. Large stick deflections are often the result of correcting for disturbances, while

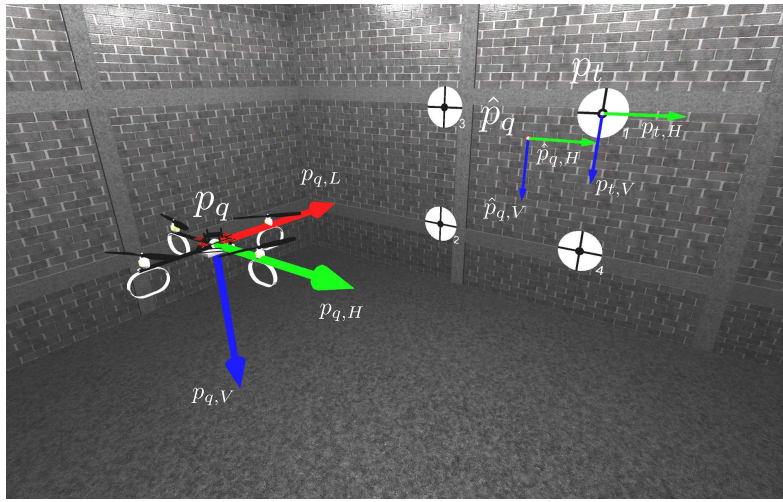

Figure 2.4: Quadrotor reference frame p_q, projected quadrotor frame $\hat{p}_q$, and target reference frame p_t. The longitudinal, lateral, and vertical components are depicted using a red, green, and blue arrows respectively.

small deflections often relate to corrective control inputs, e.g., due to drift. Therefore, this measure effectively allows to compare the disturbance rejection capabilities of the operator under different conditions.

In addition to the RMS of the stick deflection we calculated the RMS of the stick deflection velocity. Analogous to the definition of the RMS of stick deflection we calculated the RMS of stick deflection velocity for both control inputs (eq. 2.9),

$$\mathrm{RMS}_{\dot{c}} = \sqrt{\sum_{i=1}^{n} \frac{1}{n} (\dot{\alpha}_i^2 + \dot{\beta}_i^2)} \tag{2.9}$$

Table 2.2: Results of repeated measures Analysis of Variance (ANOVA) for the various measures

Measure		Result	
		$F(4, 28)$	Sig.
Accumulated error	Err_D	17.091	$p < 0.001$
Vertical accu. error	Err_V	8.353	$p < 0.001$
Horizontal accu. error	Err_H	22.513	$p < 0.001$
RMS stick deflection	RMS_c	13.717	$p < 0.001$
RMS cyclic defl.	RMS_α	18.422	$p < 0.001$
RMS collective defl.	RMS_β	3.891	$p < 0.05$
RMS stick defl. velocity	$\text{RMS}_{\dot{c}}$	18.565	$p < 0.001$
RMS cyclic defl. vel.	$\text{RMS}_{\dot{\alpha}}$	24.036	$p < 0.001$
RMS collective defl. vel.	$\text{RMS}_{\dot{\beta}}$	8.045	$p < 0.001$

the cyclic stick (eq. 2.10), and the collective lever (eq. 2.11).

$$\text{RMS}_{\dot{\alpha}} = \sqrt{\sum_{i=1}^{n} \frac{1}{n} \dot{\alpha}_i^2} \tag{2.10}$$

$$\text{RMS}_{\dot{\beta}} = \sqrt{\sum_{i=1}^{n} \frac{1}{n} \dot{\beta}_i^2} \tag{2.11}$$

2.7 Results

We tested 8 participants aged between 23 and 36 and with normal or corrected-to-normal vision. The results of the repeated measures Analysis of Variance (ANOVA) for the individual measures are summarized in (Table 2.2). Post hoc tests with Bonferroni correction for multiple comparisons were used to reveal differences between conditions.

The statistical analysis is divided into two parts. In the first part we analyzed the mean accumulated error per condition across participants. In the second part we analyzed the control activity of the participants.

Since we were interested in the effects of motion feedback on the accumulated error and control activity, all comparisons and reported significant differences are with respect to the no-motion condition.

Fig. 2.5 shows the mean accumulated error per condition, averaged across participants. Post hoc tests revealed that the accumulated error of the distance (Err_D) in condition $(0.0, 0.0)$ is significantly higher than in conditions $(0.2, 0.1)$, $(0.2, 0.2)$, and $(0.4, 0.2)$, which do not differ from each other.

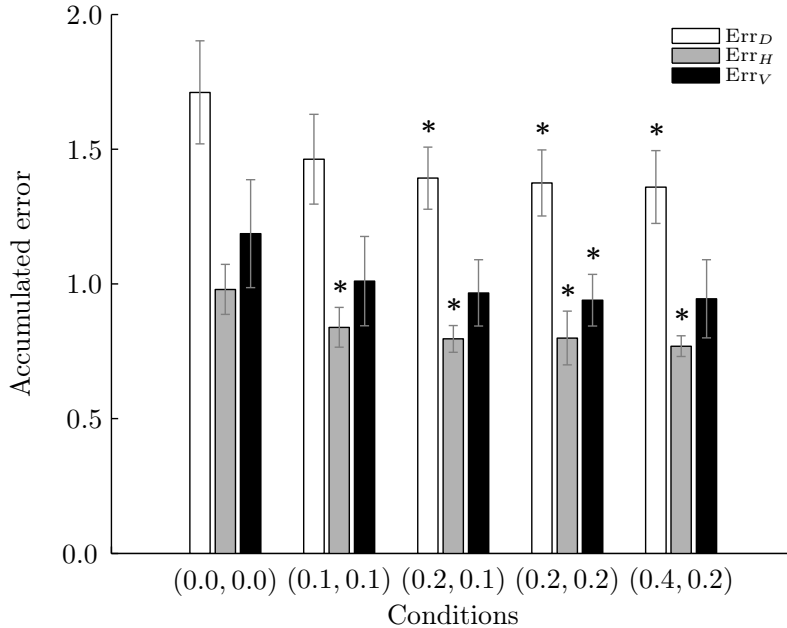

Figure 2.5: Bars denote the mean accumulated error per condition with the white bar representing the full error distance to the target, the gray bar only the horizontal and the black bar only the vertical component. Error bars: 95% CI (after correcting for mean deviation). Numbers in parentheses refer to the condition and indicate lateral and vertical motion scaling factors.

This indicates that hovering was more precise when motion feedback was presented, independently of the scaling. We also found

no significant difference between conditions with motion feedback, indicating that increasing the motion feedback scaling does not further reduce the accumulated error. Moreover, nonuniform motion scaling between lateral and vertical motion shows no difference to uniform scaling of the vehicle state. We conclude that variations in motion scaling gain, even in a nonuniform way, result in increased hover performance.

Post hoc tests on accumulated horizontal error (Err_H) revealed that the accumulated error in condition $(0.0,\ 0.0)$ is significantly higher than all other conditions, which do not differ from each other.

Post hoc tests on accumulated vertical error (Err_V) revealed that the accumulated error in condition $(0.2,\ 0.2)$ is significantly lower than condition $(0.0,\ 0.0)$. All other conditions do not differ from each other.

The analysis of the horizontal accumulated error Err_H showed that all conditions that included motion feedback produce a significantly lower error than the no-motion condition $(0.0, 0.0)$. However, the analysis of Err_V did not show this pattern and only condition $(0.2, 0.2)$ showed to be significantly lower compared to the no-motion condition, but this is not a systematic effect, since it did not show in other conditions. We conclude that the overall performance is mainly due to the performance increase in the horizontal direction. Since the disturbance signal only acted horizontally we further conclude that the improvement in hovering may be a result of an improvement in rejecting the disturbance signal.

In the second part of the analysis the focus is set on the changes of the control input given by the operator under different conditions. Fig. 2.6a shows the RMS of the stick deflection per condition, averaged across all participants. Post hoc tests of RMS_c, which includes both the deflection of the collective and the roll control stick, revealed that the RMS in condition $(0.0,\ 0.0)$ is significantly lower than in conditions $(0.1,\ 0.1)$, $(0.2,\ 0.1)$, and $(0.2,\ 0.2)$, which do not differ from each other.

Post hoc tests of RMS_α, representing the RMS of the roll control stick deflection, revealed that the RMS in condition $(0.0,\ 0.0)$ is

significantly lower than in all other conditions, which do not differ from each other.

The mean RMS of the collective control stick (RMS_β) averaged across all participants showed no significant difference between conditions in the post hoc tests.

Therefore, we conclude that the increase in RMS_c is due to the increase in RMS_α. Since the disturbance only acted on the lateral motion of the quadrotor, we further conclude that the increase of RMS_α is linked to the disturbance rejection behavior of the participants.

Fig. 2.6b shows the RMS of the stick deflection of all participants per condition. Post hoc tests of $RMS_{\dot{c}}$, which includes both the deflection velocity of the collective lever and the cyclic control stick, revealed that the RMS in condition $(0.0, 0.0)$ is significantly lower than all other conditions. We found a significant difference between conditions $(0.1, 0.1)$ and $(0.2, 0.2)$ and between $(0.2, 0.1)$ and $(0.2, 0.2)$. Note that this effect is not present in the RMS of stick deflection RMS_c. We believe that this is not a systematic effect, but due to the small amount of subjects the data does not provide conclusive evidence with respect to the source of this observation.

Post hoc tests revealed that the RMS of the cyclic stick ($RMS_{\dot{\alpha}}$) in condition $(0.0, 0.0)$ is significantly lower than in all other conditions, which do not differ from each other. The post hoc tests of $RMS_{\dot{\beta}}$ showed no significant difference between the conditions. We argue that the increase in $RMS_{\dot{c}}$ is due to the increase in stick deflection velocity of the cyclic stick $RMS_{\dot{\alpha}}$. Again, since only lateral disturbances were present in this experiment, we conclude that the increase of $RMS_{\dot{\alpha}}$ is linked to the disturbance rejection behavior of the participants.

2.8 Implication of motion feedback on hover performance

In this experiment participants were asked to hover in front of a series of targets while experiencing different types of motion feedback conditions. The results show that the accumulated error is

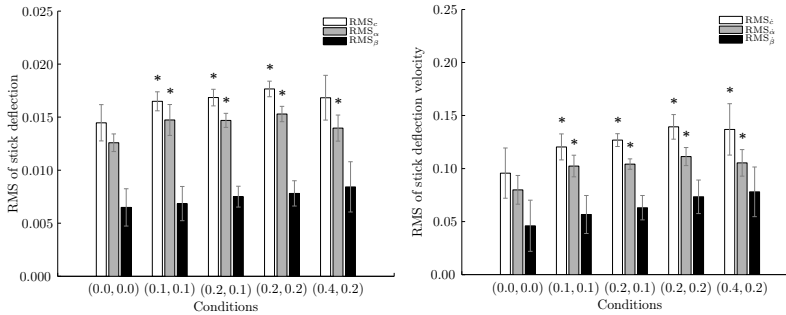

(a) Bars denote the mean RMS of stick deflection of both control sticks (white), the cyclic stick (gray), and the collective lever (black). Error bars: 95% CI (after correcting for mean deviation). Numbers in parentheses refer to the condition and indicate lateral and vertical motion scaling factors.

(b) Bars denote the mean stick deflection velocity of both control sticks (white), the cyclic stick (gray), and the collective lever (black). Error bars: 95% CI (after correcting for mean deviation). Numbers in parentheses refer to the condition and indicate lateral and vertical motion scaling factors.

Figure 2.6: RMS of stick deflection and stick deflection velocity

decreased in conditions with motion feedback compared to no motion feedback. Therefore, including motion feedback in teleoperation hover tasks increased precision and with it may increase operation safety. Furthermore, this could increase the scope of environmental working conditions in which teleoperation can be effectively performed.

A possible explanation is that vestibular information is processed faster, compared to visual information, which could lead to increased control performance. This would be in line with the results of Hosmann, Pool et al., and Zaal et al. [Hosman, 1996; Pool et al., 2008; Zaal et al., 2009]. In their work a series of experiments that included disturbance rejection tasks have been conducted. In the presented experiments the tracking error and the user input have been recorded. Their results show a significant decrease of the tracking error in conditions that included motion feedback. They argue that the reduced perceptual latency of the vestibular system

generates a superior lead compared to the visual system. In short, the observed reduction in accumulated error may be explained by the short latency of vestibular processing compared to visual processing.

Moving from the accumulated error to the analysis of the inputs of the participants, we found that in combination with the reduction of accumulated error, the RMS of the input increases. Two different control paradigms could explain these changes. The increase in stick deflection may be due to slow movements of the cyclic stick with smaller deflections or due to fast movements with large deflections. Therefore, we analyzed the RMS of the deflection velocities $\mathrm{RMS}_{\dot{c}}$, the cyclic deflection velocities $\mathrm{RMS}_{\dot{\alpha}}$, and the collective deflection velocities $\mathrm{RMS}_{\dot{\beta}}$. The results show that $\mathrm{RMS}_{\dot{c}}$ and $\mathrm{RMS}_{\dot{\alpha}}$ are increased in conditions with motion feedback compared to the no-motion condition. We argue that participants increased their control gain resulting in faster and larger stick deflections.

In Fig. 2.6a and Fig. 2.6b a small, yet non-significant, increase in the collective deflection and collective deflection velocity can be seen. This result can be explained with the collective input being dependent on the cyclic input. Given a nonzero cyclic input, the quadrotor starts to tilt and the vertical component of the thrust, opposing the acceleration due to gravity, is reduced. In order to maintain height, this needs to be compensated by increasing the thrust input using the collective lever. With an overall increase of cyclic deflection and cyclic deflection velocity, an increased collective deflection and collective deflection velocity can therefore be expected.

The experimental setup described in this work has some similarities to the setup used by Robuffo Giordano et al. [Robuffo Giordano et al., 2010]. In both experimental setups, participants controlled a remote quadrotor in order to complete a series of hover tasks.

However, the results of [Robuffo Giordano et al., 2010] did not show an increase in performance in motion feedback conditions. When comparing the stick deflection, we see an increase in motion feedback conditions in our work, while in [Robuffo Giordano et al., 2010] a decrease in stick deflection in conditions with motion feedback was measured.

We believe that this may be an effect of the MDA used by Robuffo Giordano et al. The MDA was designed to expand the motion envelope of the CMS by mapping lateral motion to a cylindrical motion. However, this may have caused participants to perceive false rotational cues that did not match with the visual feedback. These cues may have been less informative than the lateral motion cues provided by exploiting the simulators linear axis used in this experiment.

The wind disturbance signal acted only on the lateral motion of the quadrotor. As a result participants were forced to constantly correct the position of the remote vehicle. In conditions that included motion feedback we see that participants were able to reduce the accumulated error. The source of the improvement is the reduced horizontal accumulated error. In addition, the stick activity increased leading to larger and faster control inputs. The source of increased stick activity is the cyclic stick, which is controlling the lateral motion of the quadrotor. We therefore conclude that the improvement in hovering may be the result of an improvement in rejecting the disturbance signal.

The results of this experiment show that providing motion feedback increases the control performance. Participants were able to better reject disturbances, resulting in a higher precision in controlling the vehicle. Participant performance in conditions with nonuniform feedback scaling showed the same results as in conditions with uniform scaling of the lateral and vertical motion. Hence, this experiment showed that motion feedback scaling does not necessarily need to be uniform and that even with small scaling gains, e.g., $(0.2, 0.1)$, performance increases can be observed. Since teleoperated vehicles are usually not designed to carry the operator, this increases the liberty of how motion feedback may be shaped.

In this experiment motion feedback consisted of linear motion in lateral and vertical directions and roll rotation. However, it is unclear how large the individual contributions of the rotational and the linear components to the performance improvements are. In a future experiment the influence of the individual components of the motion feedback, i.e., linear and rotational motion, on the operator performance could be explored.

Chapter 3
Effects of vehicle- and task-related motion feedback on operator performance in teleoperation

3.1 Can spatial decoupling be utilized to improve performance?

Teleoperation is the control of a vehicle from a remote location. Specific to teleoperation is the spatial decoupling between the operator and the vehicle. Generally, the operator is not able to directly perceive the actions of the remote vehicle. Instead, the information needed to control the remote vehicle is transmitted using multiple communication channels. Teleoperation of a remote vehicle is therefore a challenging task. The difficulties arise from the limitations of the vehicle to carry and power sensors, and from the limitations of communication channels, which can introduce noise and delays. In addition, the information needs to be presented in a meaningful way to the operator. The loss of information that is inevitably caused by recording, processing, transmitting, and displaying data may lead to loss of situational awareness, reduced operator performance and – in the worst case – a loss of the remote vehicle.

Typically, teleoperation setups do not provide motion feedback about the state of the remote vehicle. In previous work [Lächele et al., 2014], presented in chapter 2 we investigated the effects of motion feedback on operator performance. In that work, participants controlled a remote quadrotor and completed a series of precision hover tasks. Inertial motion feedback was presented in addition to

visual feedback, where participants saw the live video stream of a camera attached to the frame of the quadrotor. The results showed a significant increase in operator performance in conditions with inertial motion feedback, although the inertial feedback was scaled (factors ranged from 0.1 to 0.4). The conclusion was that already a small amount of motion is sufficient to achieve better performance and larger feedback scaling factors do not necessarily lead to further increased performance.

In previous work [Lächele et al., 2014], see also chapter 2 participants had to compensate for external disturbances during a precision hover task. Simulated wind gusts acted on the vehicle causing the vehicle to move laterally. We hypothesized that by perceiving disturbances due to the motion feedback participants were better able to reject the disturbances. The increased disturbance rejection capabilities lead to increased hovering performance in the precision hover task. Since participants were able to better perceive the accelerations through the physical motion feedback, they were able to better correct for the errors introduced by the wind gusts, compared to visual only feedback. This is in line with previous work in vehicle simulation [Hosman, 1996; Zaal et al., 2006, 2009], where it was shown that participants were able to better reject external disturbances induced in a tracking task. Due to the design of quadrotors, commanded lateral motion always consists of two components, a roll rotation followed by a linear acceleration in the direction of roll. In the previous work the increase of performance could not be related to the individual components of this motion.

In teleoperation there is a spatial decoupling between the operator and the vehicle, this grants a certain freedom in how motion feedback can be implemented. Since the operator is not controlling from onboard the vehicle, representing the motion of the vehicle as realistic as possible becomes less important. In this work we want to investigate whether motion feedback, which contains additional information about the task, affects the operating performance in a precision hover task.

Here we present two experiments. In the first experiment, we studied the effects of including different components of the quadrotor motion in the motion feedback during the execution of precision

hover tasks. This type of motion feedback will be referred to as "vehicle-related" motion feedback. Understanding which components of the quadrotor motion can be included in the motion feedback to improve task performance would allow for "shaping" the motion feedback to be most beneficial to the operator.

In the second experiment, we elaborate this concept by introducing motion feedback that does not directly represent the motion of the quadrotor. Instead, we provide motion feedback that includes information about the task of the experiment. In these conditions, referred to as "task-related" motion feedback, the operator is presented with a roll motion that represents the offset between the actual vehicle position and the desired position in front of the target. The larger the lateral displacement of the vehicle with respect to the target, the larger the roll motion provided to the operator.

The work described in this chapter has been published in:

Lächele, J., Pretto, P., Venrooij, J., and Bülthoff, H., "Effects of vehicle- and task-related motion feedback on operator performance in teleoperation," *AHS International 72th Annual Forum*, May 2016.

3.2 Operator control station

In this teleoperation setup, operators were controlling the remote quadrotor from within a cabin that is part of the CyberMotion Simulator (CMS), see Fig. 3.1. The CMS is a motion simulator based on an industrial robot arm[a] that has been modified to increase the motion envelope of the simulator. It is mounted on a linear track, allowing for wide range of linear motion. In addition, the first rotational axis has been modified to enable for continuous rotations. The cabin of the CMS is attached by a linear rail, further increasing the range of possible motion. A detailed description of the CMS can be found in [Nieuwenhuizen and Bülthoff, 2013].

The cabin effectively shields operators from all external influences. The frontal part of the cabin can be opened to allow the operator to enter the cabin. In addition it acts as a curved screen for the projection system that is part of the cabin.

[a]KUKA GmbH, Germany

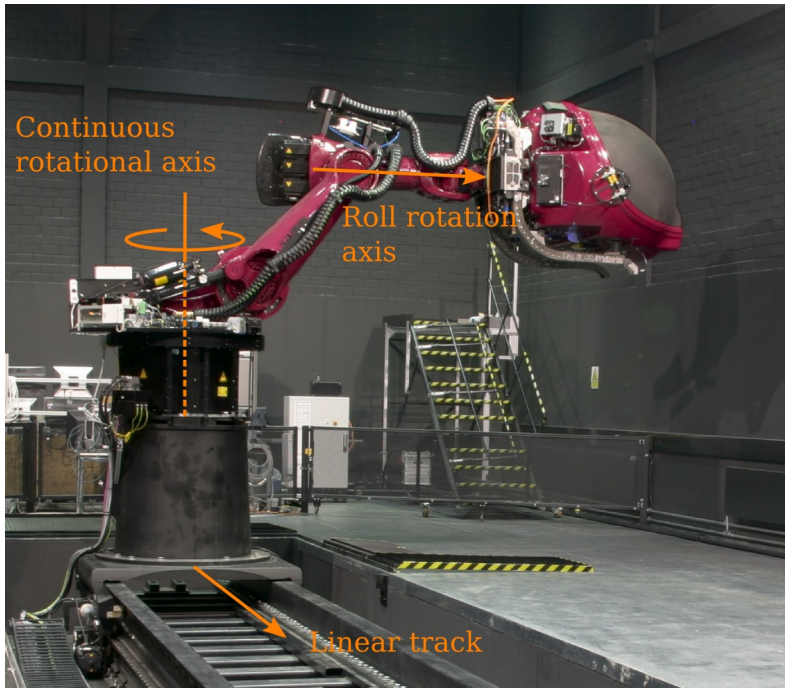

Figure 3.1: The CyberMotion Simulator (CMS) with cabin, mounted on a linear track.

The operator can control the quadrotor using a cyclic stick[b] mounted in front of the seat. Pitch input was not needed in this experiment; we therefore locked movements of the pitch axis. The stick implemented a mass-spring-damper dynamics. Movements resulted in a counteracting force consisting of an inertia component (mass), a speed-dependent component (damper) and a position-dependent stick-centering component (spring).

[b]Wittenstein AG, Germany

3.3 Virtual environment

Operators control a simulated quadrotor. Both the quadrotor and the environment are implemented using the game development engine Unity3D[c]. To achieve a physically realistic quadrotor behavior we followed a modeling approach similar to [Bouabdallah et al., 2004; Hua et al., 2009], with the rigid body dynamics simulated using Unity3D. The operator sees the environment via a virtual camera attached to the simulated quadrotor frame.

Fig. 3.2 shows screenshots of the virtual environment from the point of view of the operator in normal (Fig. 3.2a) and degraded visual condition (Fig. 3.2b). Fig. 3.2c provides an overview of the remote environment with the position of the quadrotor, the circular main target, and the green sub-targets in the scene, i.e., green lines on either side of the main target.

Fig. 3.2c provides also an overview of the degrees of freedom of a quadrotor. Using the cyclic stick the operator defines a desired roll rotation. A rotation of the quadrotor body leads to an acceleration in the direction of roll. Therefore, lateral motion is always a combination of a rotation and a resulting acceleration in the direction of roll. All other degrees of freedom were not pilot-controlled and set to a fixed value by the simulation environment.

Attached to the simulated quadrotor is a virtual camera that provides the visual feedback of the scene. However, all rotations of the quadrotor frame were compensated by a counter-rotation of the camera. As a result the position of the horizon in the camera image stays constant with respect to the head of the operator. This was done to simulate a gimballed camera system that many quadrotor systems are equipped with. In addition, this reduced the risk of the operator experiencing symptoms of motion sicknes [Oman, 1990].

3.4 Motion feedback

Following the definition of reference frames shown in Fig. 3.2c, p_t defines the position of the target in world frame. The position of the

[c]Unity Technologies, United States

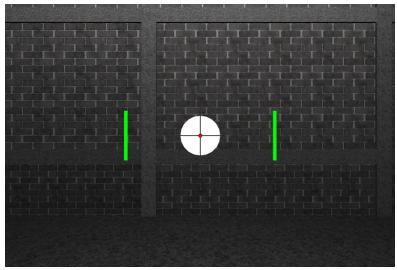

(a) Participants perspective of the onboard camera feedback

(b) Visual feedback in degraded visual conditions

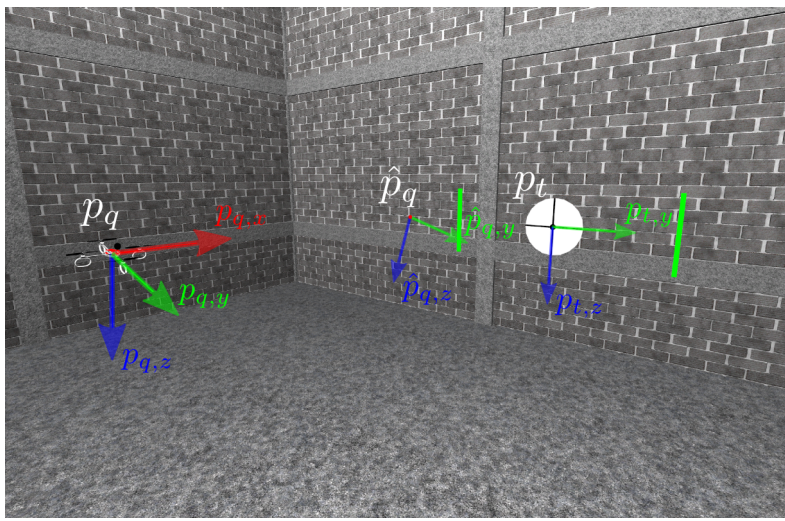

(c) Simulated quadrotor located in remote environment with reference frames.

Figure 3.2: Virtual environment used in the two experiments. Participants were able to control lateral motion of quadrotor only and were provided visual and inertial motion feedback.

quadrotor is denoted with p_q and the orthogonal projection onto the plane where the target resides is denoted with $\hat{p}_q$. The task-related motion feedback (Task), i.e., a roll motion x_{η_x}, can be expressed with (eq. 3.1).

$$\begin{aligned} x_{\eta_x} &= -\beta \underbrace{\left(p_{t,y} - \hat{p}_{q,y}\right)}_{\text{lateral offset}} \\ x_{\dot{\eta}_x} &= -\beta \underbrace{\left(\dot{p}_{t,y} - \dot{\hat{p}}_{q,y}\right)}_{\text{change in offset}} \end{aligned} \tag{3.1}$$

With β being a unitless scaling parameter that defines the sensitivity of the motion feedback towards the offset between quadrotor position and the target. In the experiments we defined $\beta = 0.3$ so that the operator is at maximum roll rotation when the quadrotor is approximately at the position of the sub-targets. Large rotations have been limited to $\pm 30°$ to avoid uncomfortable motion. The vehicle-state lateral (Lat) and vehicle-state roll (Roll) motion feedback were defined as the scaled lateral and roll motion of the remote vehicle with a scaling factor of $\alpha = 0.4$.

In addition to modifying the type of motion feedback we also modified the quality of the visual feedback (Vis). In the normal case (Vis-Hi) the rendered scene was presented in an unaltered fashion, no rendering filters were applied. In the degraded visual quality case (Vis-Lo), we applied a series of rendering filters with a negative impact on visual quality, i.e., noise, gaussian blur, motion blur, and vignetting. Fig. 3.2b shows the effects of these filters compared to Vis-Hi conditions (Fig. 3.2a).

3.5 Disturbance signal

We simulated lateral wind gusts that acted on the body of the quadrotor. These caused the quadrotor to accelerate laterally to either side in an unpredictable manner, but they did not act on roll rotation. The applied forces were calculated using the following equation.

$$F_D(t) = \frac{1}{2}\rho C_D A \cdot (V(t) - \dot{y})^2 \tag{3.2}$$

Table 3.1: Frequencies and phase shifts used for multi-sine wind disturbance signal

Index i	Frequency f_i [Hz]	Phase φ_i [rad]
1	0.0300	2.5031
2	0.1378	1.4353
3	0.2456	−0.5854
4	0.3533	2.754
5	0.4611	−1.5367
6	0.5689	0.2084
7	0.6767	2.8573
8	0.7844	−1.4593
9	0.8922	−1.5703
10	1.0000	2.6871

The reference area $A = 0.25\,\mathrm{m}^2$, the drag coefficient $C_D = 1.05$ of the vehicle and the density $\rho = 1.2\,\mathrm{kg\,m}^{-3}$ of the surrounding air were assumed to be constant throughout the experiment. This is equivalent to the drag of a cube with a surface area of $0.25\,\mathrm{m}^2$. Although this is a simplification of the actual drag of the quadrotor, the resulting forces acting on the quadrotor are realistic enough for this experiment. An in-depth derivation of (eq. 3.2) can be found in [Ruijgrok, 1996].

Wind gusts were active throughout the trials and participants had to constantly correct for the disturbances. The wind velocity signal $V(t)$ at time t was defined as a multi-sine signal consisting of 10 frequencies (f_i) with 10 phase shifts (φ_i), listed in table 3.1.

$$V(t) = \sum_{i=1}^{10} \sin\left((2\pi f_i t) + \varphi_i\right) \tag{3.3}$$

In the first experiment we investigated how the individual motion components of the quadrotor, i.e., vehicle-related roll and lateral motion, impacts the flight performance of the operator. In the second experiment, we investigated how task-related roll motion influences the flight performance of the operator. The experimental conditions for the first experiment were defined as the combination

of lateral motion present (Lat-On) or absent (Lat-Off), vehicle-related roll motion present (Roll-On) or absent (Roll-Off), and visual quality normal (Vis-Hi) or degraded (Vis-Lo), for a total of 8 conditions.

For the second experiment we followed the same experimental design, i.e., three factor, two levels each. However, we exchanged the vehicle-related roll motion (Roll) with task-related motion feedback. This was defined as task-related motion present (Task-On) or absent (Task-Off). In the task-related motion feedback conditions, operators are rolled according to the lateral offset between the quadrotor and the target position. The further to the left (or right) of the target, the further operators will be rotated to the left (or right).

3.6 Experiment description

The experimental task was to hover in front of the main target, i,e., the black inner circle of the white disk, as precise as possible for a duration of 20 s. Before starting with the main hover task, participants first had to reach two sub-targets, i.e., green vertical bars on either side of the main target. The order of reaching those could be chosen freely. The purpose of including the sub-targets was to force participants to move the quadrotor, allowing them to recognize the type of motion feedback at the start of each trial.

When the CMS reached the start position of the experiment a message was shown to the participants and they were free to start by pressing a button on the cyclic stick. Participants were able to self-initiate all the experimental trials. After completing a trial the CMS moved back again to the start position and the cycle repeated until participants requested a break or the end of the experiment was reached.

In the beginning of a trial a red dot was visible on the virtual wall in front of the operator (Fig. 3.2c) that indicated the position of the quadrotor. After having reached the two sub-targets, the precision hover began when the red indicator reached the black inner circle of the main target (see Fig. 3.2a). At this moment the red indicator disappeared in order to increase the difficulty in completing the task purely visually. During the hover task a series of beeps was audible

for the participant, indicating the remaining time to complete the trial.

Before starting the experimental trials, all participants completed a set of 48 training trials. The training was defined to introduce participants to the control task and the motion feedback. Training started with trials where only visual feedback was presented, to familiarize participants with the control task. Then gradually motion feedback conditions were presented where the scaling of the motion feedback was 50 % of the scaling of the experimental trials. The final 8 training trials consisted of all experimental conditions in a consecutive order, with no scaling.

In summary, in both experiments we followed a three factors, two levels, full-factorial design with the order of conditions chosen at random. For each condition, participants completed 12 repetitions, before proceeding with the next condition. In total participants completed 96 trials. Every 24 trials participants had a small break, but were also free to have a break whenever needed. We measured the accumulated error, i.e., the sum over time of the offset between desired and actual position of the quadrotor while the operator performs the precision hover task. The accumulated error provides a measure for the overall control performance of the operator.

$$\mathrm{Err}_D = \int \|p_t - \hat{p}_q\| \, \mathrm{d}t \tag{3.4}$$

The distance between the target (p_t) and the projected quadrotor position ($\hat{p}_q$), i.e., the position error, is then used to calculate Err_D ((eq. 3.4)). The reference frames in Fig. 3.2 show where the individual frames are located in the virtual environment.

In addition, we measured the stick deflection α of the cyclic stick. With this we calculated the root mean square of the stick deflection (RMS_α) as described in (eq. 3.5), as an indicator for the control effort of the participant.

$$\mathrm{RMS}_\alpha = \sqrt{\sum_{i=1}^{n} \frac{1}{n} \alpha_i^2} \tag{3.5}$$

By incorporating squared values into the measure, the RMS suppresses smaller values, often related to corrective control inputs,

while at the same time reinforcing the influence of large control inputs, often the result of correcting for disturbances. Therefore, this measure effectively allows to compare the disturbance rejection capabilities of the operator under different conditions.

In total 23 paid participants voluntarily joined the experiments. 10 participants (3 female) in the first experiment and 10 (1 female) in the second. Three participants did not finish the experiment (One in the first, two in the second experiment), due to mild symptoms of motion sickness. All participants had normal or corrected-to-normal vision.

We used three-way ANOVAs to test the statistical significance of differences in the measurements, with participant defined as a random factor. This is mathematically equivalent to a repeated-measures ANOVA. For the post hoc comparisons of means, we used Bonferroni corrections.

3.7 Results

The results of the first experiment can be seen in Fig. 3.3. The top row of figures shows the accumulated error (Err_D) for the visual quality (Vis), the lateral motion feedback (Lat), and the roll motion feedback (Roll) factors. The bottom row shows the effects of the same three factors on the stick deflection (RMS_α).

An ANOVA determined that the accumulated error (Err_D) differed significantly for visual quality (Vis) ($F(1,949) = 443.43, p < 0.001$) and lateral motion feedback (Lat) ($F(1,949) = 190.51, p < 0.001$). Post hoc tests using the Bonferroni correction revealed a significant increase in accumulated error (Err_D) in reduced visual quality conditions (Vis-Lo) (Fig. 3.3a) and a significant reduction for Err_D when lateral motion feedback was provided (Lat-On) (Fig. 3.3b). We found no significant differences between roll motion feedback conditions (Roll-On) and not providing roll motion feedback (Roll-Off) (Fig. 3.3c).

In addition, an ANOVA revealed a significant effect of visual quality ($F(1,949) = 500.63, p < 0.001$) and roll motion feedback ($F(1,949) = 13.54, p < 0.001$) on the average stick deflection (RMS_α),

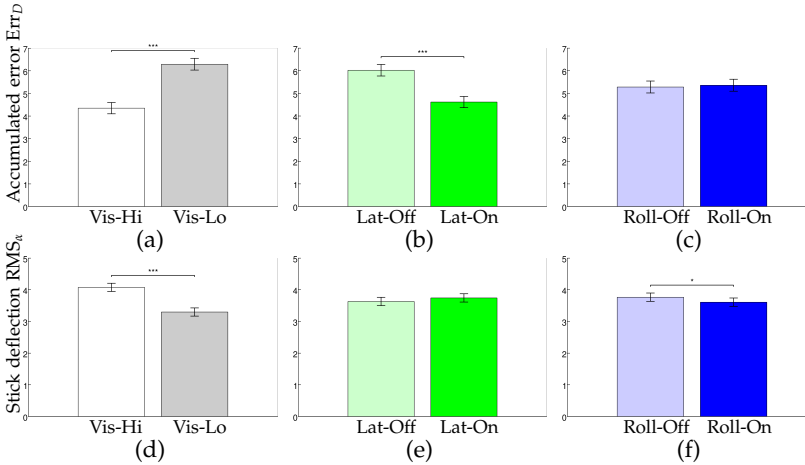

Figure 3.3: Main effects of the first experiment for accumulated error (top row) and stick deflection (bottom row) for 10 participants. Error bars denote ± 1 standard error. First column represents visual quality (Vis), second column lateral (Lat), and third column roll (Roll) motion feedback conditions.

Post hoc test using Bonferroni correction revealed a significant decrease of RMS_α in reduced visual quality (Vis-Lo) conditions (Fig. 3.3d) and when roll motion feedback was provided (Fig. 3.3f).

The results of the second experiment can be seen in Fig. 3.4. It shows the average accumulated error over 10 participants. An ANOVA determined a significant effect of visual quality (Vis) ($F(1,949) = 389.94, p < 0.001$), lateral motion feedback (Lat) ($F(1,949) = 121.94, p < 0.001$), and task-related (Task) motion feedback ($F(1,949) = 57.30, p < 0.001$) on the accumulated error (Err_D). Post hoc comparisons using Bonferroni corrections for multiple comparisons revealed a significant increase in Err_D in degraded visual quality (Vis-Lo) conditions (Fig. 3.4a), and significant reductions when lateral (Lat-On) (Fig. 3.4b), and task-related (Task-On) motion feedback (Fig. 3.4c) was provided.

We found an interaction between the lateral (Lat) and task-related (Task) motion feedback conditions. The improvements due to providing lateral motion feedback is larger when no task feedback

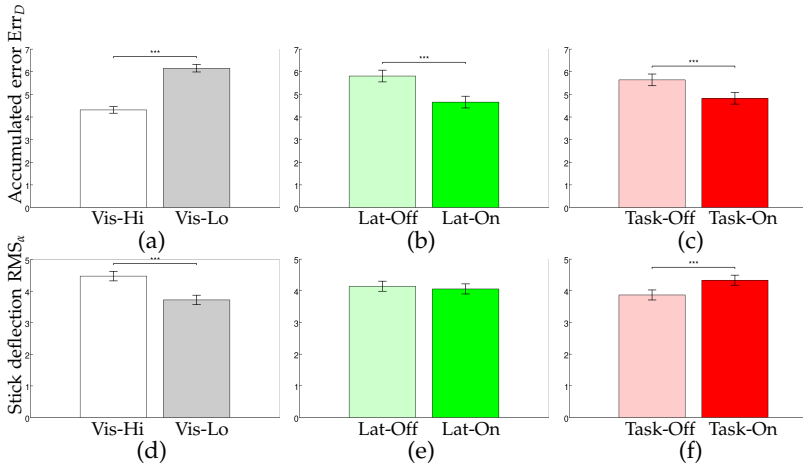

Figure 3.4: Main effects of the second experiment for accumulated error (top row) and stick deflection (bottom row) for 10 participants. Error bars denote ± 1 standard error. First column represents visual quality (Vis), second column lateral (Lat), and third column roll (Roll) motion feedback conditions.

is provided. In conditions that include task-related motion feedback, the additional lateral motion feedback resulted in only small improvements. This could be a ceiling effect where participants already performed at a level where no further improvements can be expected.

The results for the RMS_α measure for the second experiment are shown in Fig. 3.4. An ANOVA determined a significant effect for visual quality (Vis) ($F(1,949) = 249.42, p < 0.001$) and task-related motion feedback (Task) ($F(1,949) = 82.24, p < 0.001$). Post hoc tests with Bonferroni corrections revealed a significant reduction for RMS_α in degraded visual feedback conditions (Vis-Lo) (Fig. 3.4d) and a significant increase when task-related motion feedback (Task-On) was provided (Fig. 3.4f).

3.8 Applicability of tasks describing motion feedback

In both experiments we observe a clear negative influence of degraded visual quality on operator performance. This was expected, since several previous studies found similar results in experiments where operators controlled a vehicle. One can refer to [Chen et al., 2007; Pretto et al., 2012] for an extensive overview of different influences and how they affect performance. The task presented in this experiment heavily relies on visual feedback, therefore, reducing the quality of the feedback, i.e., reducing the amount of visual information in the feedback, leads to reduced performance.

In teleoperation wireless communication channels are used to transmit the live video stream. To reduce bandwidth it is common practice to reduce the frame rate and resolution of the video. This results in a degradation of the visual feedback, a common challenge in teleoperation. An alternative approach is the use of multiple displays providing feedback about the state of the vehicle. However, operators may not optimally use visual displays [Tvaryanas, 2004], in the absence of multisensory cues. Therefore, using additional or alternative feedback types that require less bandwidth become relevant.

Results of a previous study [Lächele et al., 2014] indicated that motion feedback has positive effects on operator performance. What is shown in addition in the current study, is that not all motion components contribute in the same way. By splitting the motion of the remote quadrotor in roll and lateral components we saw that only the lateral motion had a positive effect on performance. The explanation for the results in [Lächele et al., 2014] was that the increased performance may be due to increased disturbance rejection capabilities. With the results of this experiment we can provide additional evidence for this conclusion.

During the trials, participants perceived wind gusts that only acted on the lateral motion of the quadrotor. They did not cause any disturbances on the roll motion. Therefore, information about the disturbances is only presented in the lateral motion feedback, not in the roll motion feedback. Since performance increased in

conditions that included lateral motion feedback and did not change in conditions with roll motion feedback it follows that this increase is due to improved disturbance rejection.

Human's ability to visually detect small changes in velocity, e.g., due to the wind disturbances, is very poor [Monen and Brenner, 1994]. By providing motion feedback on these disturbances through the vestibular system, the human inertial sensors in the inner ear, operators are able to better correct for disturbances resulting in reduced Err_D. This would be in line with the results of previous studies in vehicle simulation [Hosman, 1996; Zaal et al., 2006, 2009].

Although roll motion feedback did not influence performance, we found an effect on the control effort, RMS_α. Participants showed smaller RMS_α in conditions including roll motion feedback (Roll-On), compared to Roll-Off conditions. The stick inputs define the roll angle of the quadrotor, which in turn define the lateral acceleration of the vehicle. By perceiving the roll motion and hence lateral acceleration, a feedback loop for lateral acceleration is established. This allows for a more precise control over the lateral acceleration with less input correction needed, hence reducing control effort.

On the other hand, in task-related motion feedback conditions we found a significant increase in RMS_α. This means participants had to invest more control effort to achieve higher performance compared to lateral motion feedback (Lat-On). In task-related motion feedback conditions the whole cabin of the CMS is being moved, including the participant and the cyclic control stick. This might cause involuntary stick input, leading to an increase in stick deflection RMS_α. However, the results do not allow for a final conclusion. A followup experiment could take the influence of the cabin motion into account to avoid involuntary input.

Moreover, we found a reduction of RMS_α in degraded visual feedback conditions. This can be explained by the degraded visual condition providing less information about the tracking task. This leads to poorer performance in judging the relative position and less corrections being made, hence reduced control effort. This is in line with the performance measures, where we found increased accumulated error (Err_D) in degraded visual feedback conditions (Vis-Lo).

We also found a significant interaction between the lateral and task-related motion feedback conditions. The positive effect of providing task-related motion feedback was smaller when lateral motion feedback was provided, compared to when no lateral motion feedback was provided. This may be the result of a ceiling effect, i.e., participants already achieved close to optimal performance in conditions with lateral motion feedback. Providing additional feedback then does not further improve how well participants can complete the task.

The results of this work show the benefits of motion feedback in teleoperation setups. By perceiving the inertial motion of the remote vehicle, operators are able to better reject external disturbances and improve performance. In addition, the results show that task-related inertial motion feedback can also be used by operators to improve control performance. Exploiting the spatial decoupling between the operator and the vehicle allows for shaping motion feedback, creating the possibility to provide optimal motion feedback depending on the task and the vehicle. Future experiments could explore the application of task-related motion feedback in different teleoperation scenarios with a range of different tasks.

Chapter 4

Novel approach for calculating motion feedback in teleoperation

4.1 Can motion feedback be shaped to benefit teleoperation?

Teleoperation is the control of a system by a human operator from a remote location. Specific to teleoperation is the spatial decoupling between the location from where an operator is controlling the system and the location or environment where the vehicle is moving and acting in. Therefore, in teleoperation the operator does not directly perceive the state of the remote vehicle. Three parts are essential for teleoperation: a vehicle equipped with the necessary devices to sense and operate in the remote environment, a control station that includes control devices and displays information of the vehicle in a meaningful way to the operator. Finally, bidirectional communication channels, capable of transmitting the information from the vehicle to the operator and from the operator the control commands back to the vehicle.

The type of vehicle used in a teleoperation setup depends mainly on the task. Transportation and disposal tasks are often performed by ground robots, as the payload can usually be heavier and larger compared to aerial vehicles. Search and rescue, inspection, and surveillance tasks are often performed by aerial vehicles as they can provide the necessary overview and are able to quickly change their perspective on points of interest. In addition, aerial vehicles like multirotors can hover, which is beneficial for acquiring an overview.

Teleoperation of remote vehicles is known to be difficult. The challenges arise by the limitations of the remote vehicle (e.g., power consumption, weight), noise of the sensors, and the delays and noise introduced by the transmission. These issues increase the chance of loss of situational awareness of the operator resulting in problems ranging from reduced operating performance to a complete loss of the remote vehicle. One way to cope with the challenges is to increase the autonomy of the remote vehicle. With the help of on-board GPS, speed sensors, etc. autonomous flight controllers can be implemented. This allows the operator to define waypoints that are reached by the on-board controller instead of controlling the vehicle itself to reach those waypoints. However, in some environments, e.g., indoor environments, positioning sensors, like GPS, become unreliable or fail and this approach no longer works. Another approach is to improve how information is being presented to the operator. Traditional teleoperation setups usually include one or more visual feedback channels. However, visual feedback commonly has limitations that have a deteriorating effect on the control performance. Chen et al. [Chen et al., 2007] provide an in-depth discussion about a range of effects like limited field of view, large time delays, low framerate, and noise and how they affect performance.

In this work we focus on teleoperation of an octorotor, since it can perform a variety of tasks while at the same time is able to carry a reasonable amount of payload, e.g., sensors, cameras. We present a teleoperation setup where the operator experiences visual feedback and in addition, physical motion feedback about the motion of the remote vehicle. We argue that operators incorporate the additional information in their control strategy, leading to increased situational awareness and as a result an increase in performance.

In previous studies [Hing and Oh, 2009; Ortiz et al., 2008; Robuffo Giordano et al., 2010] the possible application of motion feedback has been explored. In those studies, a motion simulator is utilized to provide feedback of the motion of the remote vehicle. Providing motion feedback with a motion simulator that benefits the operator optimally is challenging. One often used approach is using a filter-based Motion Cueing Algorithms (MCA) that provide a way to map

the vehicle motion to the limited motion envelope of the simulator. Filter-based MCA require expert tuning of the filter parameters to prevent false motion cues perceivable by the operator. These unwanted motion cues can lead to a false understanding of the remote vehicle motion by the operator leading to reduced performance. In this chapter an alternative to this approach is explored. Instead of using a MCA, we move the simulator cabin according to the scaled motion of the remote octorotor.

The work described in this chapter has been published in:

Lächele, J., Pretto, P., Venrooij, J., Zell, A., and Bülthoff, H., "Novel approach for calculating motion feedback in teleoperation," *7th European Conference on Mobile Robots*, September 2015.

4.2 Definition of motion feedback in teleoperation

One motivation to include motion feedback in a teleoperation setup is to provide useful information about the vehicle acting in the remote environment. By directly perceiving the motion of the vehicle, the operator should better understand the movements of the vehicle in the remote environment. With the increased situation awareness, an increase in task performance can be expected.

Another possibility is presented by the properties of teleoperation, i.e., the spatial decoupling between the operator and the remote vehicle. The fact that the operator is not able to directly perceive the motion of the remote vehicle grants the freedom to shape motion feedback. This allows to include additional information about the teleoperation task in the motion feedback. We hypothesize that including information about the task in the motion feedback will further help controlling the remote vehicle.

In this section we propose a general way to calculate motion feedback in teleoperation scenarios. We first define vectors that describe the motion of the remote vehicle, a desired trajectory defining an optimum to complete a task, and the actual motion of the operator that is being recreated by a motion simulator. Based on those definitions we introduce a transformation to calculate motion feedback.

We define the position and orientation introduced below with respect to the world reference frame. The cartesian position of the vehicle will be expressed by the vector $\boldsymbol{x} = \begin{bmatrix} x & y & z \end{bmatrix}^T$. The first and second time derivatives, velocity and acceleration, will be expressed as $\dot{\boldsymbol{x}}$ and $\ddot{\boldsymbol{x}}$, respectively. The orientation will be expressed as a vector with the elements being defined as the Euler angles $\boldsymbol{\eta} = \begin{bmatrix} \phi & \theta & \psi \end{bmatrix}^T$. The Euler angles follow the Z-Y-X order of application, with ψ defining the rotation around the z-axis, θ the rotation around the y-axis, and ϕ the rotation around the x-axis. The two time-derivatives $\dot{\boldsymbol{\eta}}$ and $\ddot{\boldsymbol{\eta}}$ define the velocity and the acceleration of the individual Euler angles. This should not be confused with the angular velocity $\boldsymbol{\omega}$ or the angular acceleration, usually expressed as $\boldsymbol{\alpha}$. Both do not follow the Euler definition but instead describe an axis of rotation.

The **Vehicle state** $\boldsymbol{s_v}$ describes the state of the vehicle and includes position, velocity, and acceleration for both, linear and angular motion.

$$\boldsymbol{s_v} = \begin{bmatrix} \boldsymbol{x^v} & \dot{\boldsymbol{x}}^v & \ddot{\boldsymbol{x}}^v & \boldsymbol{\eta^v} & \dot{\boldsymbol{\eta}}^v & \ddot{\boldsymbol{\eta}}^v \end{bmatrix}^T \in \mathbb{R}^{18} \tag{4.1}$$

In the same way, **target state** $\boldsymbol{s_t}$ describes a target trajectory the vehicle should follow to complete the task in an optimal way.

$$\boldsymbol{s_t} = \begin{bmatrix} \boldsymbol{x^t} & \dot{\boldsymbol{x}}^t & \ddot{\boldsymbol{x}}^t & \boldsymbol{\eta^t} & \dot{\boldsymbol{\eta}}^t & \ddot{\boldsymbol{\eta}}^t \end{bmatrix}^T \in \mathbb{R}^{18} \tag{4.2}$$

Motion feedback $\boldsymbol{s}$ describes how the operator is being moved by a motion platform.

$$\boldsymbol{s} = \begin{bmatrix} \boldsymbol{x} & \dot{\boldsymbol{x}} & \ddot{\boldsymbol{x}} & \boldsymbol{\eta} & \dot{\boldsymbol{\eta}} & \ddot{\boldsymbol{\eta}} \end{bmatrix}^T \in \mathbb{R}^{18} \tag{4.3}$$

To include both vehicle state and target state in the motion feedback, we define $\boldsymbol{s}$ as the sum of two transformations. The first transformation, **vehicle state transformation** $\boldsymbol{s_1} = A\boldsymbol{s_v}$, defines the influence of the vehicle state on the motion feedback. In the same way, the **target state transformation** $\boldsymbol{s_2} = B\boldsymbol{s_t}$, describes the influence of the target state on the feedback. Both transformations can be expressed as matrices A and B, defined in (eq. 4.4) and (eq. 4.5) respectively.

$$A = \begin{bmatrix} a_{x_x,x_x^v} & a_{x_x,x_y^v} & \cdots & a_{x_x,\ddot{\eta}_\psi^v} \\ a_{x_y,x_x^v} & a_{x_y,x_y^v} & \cdots & a_{x_y,\ddot{\eta}_\psi^v} \\ \vdots & \vdots & \ddots & \vdots \\ a_{\ddot{\eta}_\psi,x_x^v} & a_{\ddot{\eta}_\psi,x_y^v} & \cdots & a_{\ddot{\eta}_\psi,\ddot{\eta}_\psi^v} \end{bmatrix} \tag{4.4}$$

$$B = \begin{bmatrix} b_{x_x,x_x^t} & b_{x_x,x_y^t} & \cdots & b_{x_x,\ddot{\eta}_\psi^t} \\ b_{x_y,x_x^t} & b_{x_y,x_y^t} & \cdots & b_{x_y,\ddot{\eta}_\psi^t} \\ \vdots & \vdots & \ddots & \vdots \\ b_{\ddot{\eta}_\psi,x_x^t} & b_{\ddot{\eta}_\psi,x_y^t} & \cdots & b_{\ddot{\eta}_\psi,\ddot{\eta}_\psi^t} \end{bmatrix} \tag{4.5}$$

The components of A, i.e., $a_{\alpha,\beta} \in \mathbb{R}$, define scaling factors, where α refers here to a component of the motion feedback $\boldsymbol{s}$, e.g. roll η_ϕ, and β refers to a component of the vehicle state vector $\boldsymbol{s_v}$, e.g., acceleration $\ddot{x}_y^v$. Therefore, $a_{\alpha,\beta} \in \mathbb{R}$ defines how the motion feedback coefficient α depends on the vehicle state coefficient β. In the same way the individual components $b_{\alpha,\beta}$ of matrix B describe the dependency of the motion feedback coefficient α on the component β of the task state $\boldsymbol{s_t}$.

Now we can introduce the definition of motion feedback $\boldsymbol{s}$ as the sum of $\boldsymbol{s_1}$ and $\boldsymbol{s_2}$. To simplify notation, matrices A and B are combined to get the **motion feedback transformation** M and $\boldsymbol{s_v}$ and $\boldsymbol{s_t}$ are combined to yield the **vehicle-target vector** $\boldsymbol{s_{vt}}$.

$$\begin{aligned} \boldsymbol{s} &= \boldsymbol{s_1} + \boldsymbol{s_2} \\ &= A\boldsymbol{s_v} + B\boldsymbol{s_t} \\ &= \begin{bmatrix} A & B \end{bmatrix} \begin{bmatrix} \boldsymbol{s_v} \\ \boldsymbol{s_t} \end{bmatrix} \\ &= M\boldsymbol{s_{vt}} \end{aligned} \tag{4.6}$$

With (eq. 4.6) it is possible to describe any possible linear mapping between vehicle and target state to motion feedback. Specific elements of the state vectors can be scaled or discarded, depending

on the desired motion feedback. This allows to shape motion feedback to best fit the teleoperation scenario, task, or vehicle used in the setup. More specifically, (eq. 4.6) introduces the possibility to provide motion feedback that does not represent physically realistic motion.

As an example, consider mapping lateral and longitudinal accelerations of a vehicle to a rotation. For lateral accelerations the operator would be rotated around the roll axis and for longitudinal accelerations the operator would be rotated around the pitch axis. Although this type of motion feedback is not representing the physical motion of the vehicle, the motion feedback still transports the information of acceleration in a potentially meaningful way. This exploits the spatial decoupling between the operator and the vehicle and grants the freedom to define more abstract form of motion feedback. As a result, a multitude of different motion feedback definitions can be expressed by a single matrix multiplication.

4.3 Control Station

The teleoperation setup can be split into two separate environments, the remote environment where the octorotor is flying and the local control station from where the operator controls the octorotor. Notably, both environments are connected only via communication channels, the operator cannot directly perceive any information from the remote vehicle. Figure 4.1 provides an overview of the two environments with the equipment used in our teleoperation setup based on the footprint of the building where the setup is located, with the remote environment (highlighted in light yellow) and the control station in the upper part of the figure (light blue). Descriptions of the individual components can be found in the following subsections.

Our teleoperation control station is inside the cabin of the CyberMotion Simulator (CMS). The CMS is based on an industrial robot[a] that has been modified to increase the motion envelope, by a linear track, increasing the range of linear motion significantly. In addition,

[a]Manufactured and distributed by KUKA GmbH, Germany

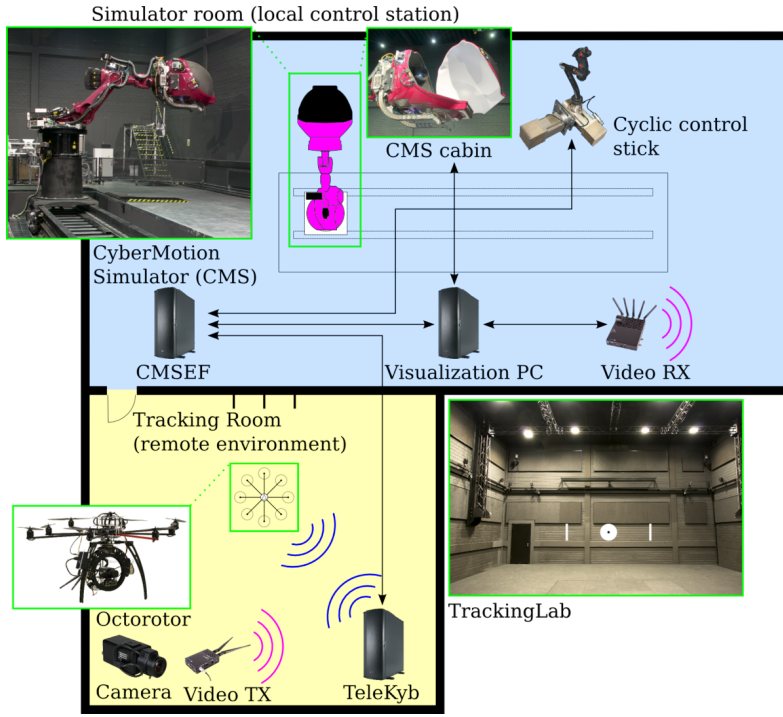

Figure 4.1: Overview of the teleoperation equipment. Black arrows denote communication channels using network connections.

the first rotational axis of the simulator has been modified to allow for continuous rotation. Finally, a cabin track connects the cabin with the rest of the CMS, further increasing the motion envelope of the simulator. Figure 4.2 shows the CMS mounted on the linear track with the cabin.

After being seated inside the cabin the operator is effectively shielded from unwanted external influences. The cabin is equipped with a projection system consisting of two projectors. The projectors provide the visual feedback using the inside of the cabin as the screen with a large field of view ($140° \times 70°$), a framerate of 60 Hz

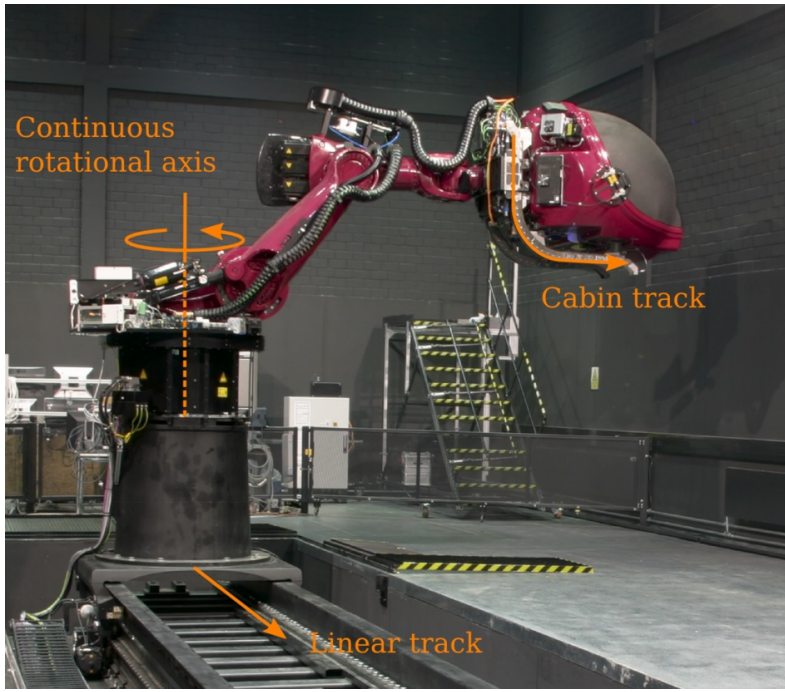

Figure 4.2: The CyberMotion Simulator (CMS) with cabin and mounted on a linear track

and a resolution of 1280 px × 720 px. A cyclic control stick and a collective lever[b] are mounted inside the cabin.

4.4 Octorotor and remote environment

The remote environment is referred to as the TrackingLab, a large tracking space located next to the hall with the CMS, where the octorotor can fly safely. The TrackingLab is equipped with an

[b]Manufactured and distributed by Wittenstein AG, Germany

optical tracking system[c] that allows objects to be tracked within a $8\,\mathrm{m} \times 8\,\mathrm{m} \times 3\,\mathrm{m}$ volume with an update rate of 120 Hz.

The real-time pose of the octorotor is used to implement a flight control program using TeleKyb [Grabe et al., 2013], a software framework based on the Robot Operating System (ROS) [Quigley et al., 2009]. TeleKyb is designed for the bilateral teleoperation of groups of multirotor Unmanned Aerial Vehicles (UAVs).

A cascaded control scheme is implemented that controls the octorotor flight. A high level control algorithm controls the position and velocity of the octorotor described by an input trajectory. It calculates commands, i.e., desired roll and pitch angles, yaw rate, and thrust. The control commands are sent to the octorotor where an on-board low level control algorithm actuates the propellers, in order to reach the desired pose.

4.5 Video system

The video camera attached to the octorotor supports multiple video formats up to full-HD format 1080p at a frequency of 30 Hz. With a lower resolution of 720p the update rate can be increased to 60 Hz.

To allow for greater control of the visual feedback the camera is attached to an active gimbal system. This system can be used to orient the camera independently of the octorotor orientation. In this setup we use the gimbal system to stabilize the camera orientation, i.e., counteracting rotations of the octorotor. As a result the horizon seen in the video stays level at all times.

Attached to the camera is a laser pointer that projects a green dot straight ahead in the center of the cameras FOV. The green dot provides a visual reference for the position of the octorotor and is continuously visible.

The live video stream of the camera mounted on the octorotor is being transmitted using a specialized wireless transmission system that utilizes several channels in the 5.8 GHz band. The receiver of the transmission system is mounted on the base of the CMS. There, the video output of the wireless video receiver is grabbed

[c] Manufactured by Vicon Motion Systems Ltd. UK

using a framegrabber PCI express card (DELTA-3G-elp 11)[d]. The framegrabber includes a software development kit (SDK) that is used to interface the grabbing hardware in order to display the extracted images of the input video stream on the projection screen of the CMS.

4.6 Experiment description

We conducted an experiment using the teleoperation setup described above. The goal of this experiment was to validate the applicability of our method for calculating motion feedback in a hardware/human-in-the-loop scenario. Furthermore, this was the first application of this setup, allowing to gain insights into how it could be improved in future applications.

The experiment starts with the participant seated in the cabin of the CMS, the CMS is in its neutral position and the octorotor on the ground. The cabin displays a message that the experiment will start soon. Using a gamepad connected to the TeleKyb computer, the experimenter starts the automated take-off of the octorotor.The octorotor will then fly to the experiment start position while the CMS moves to its experiment start position.

After both reach their start positions, a message is displayed to the operator that the trial can be started. The participant is now in control and by pressing a button on the cyclic control stick the trial begins. Only then the visuals switch to the live video feed coming from the octorotor camera and the operator is able to control the octorotor.

After completing a trial the video feed is disabled and instead, a message is displayed to let the operator know that the next trial is prepared. At the same time the octorotor re-enables automated control and flies back to the start position for the next trial, while at the same time the CMS repositions itself to its start position.

This procedure repeats until the octorotor needs to land in order to change the depleted batteries. The landing procedure is initiated by the experimenter by pressing the landing button on the gamepad.

[d]Manufactured and distributed by DELTACAST, Belgium

The landing procedure also causes the CMS to move back to the neutral position that allows the participant to leave the CMS cabin. During the exchange of batteries the participant can have a small break.

In each trial the participants complete precision hover tasks that consist of three components. First, the octorotor needs to be moved to the left or right hand side of the target in order to reach a subtarget, i.e., a white vertical stripe on the wall, as seen in the TrackingLab photograph in Figure 4.1. Participants will hear a beep that indicates when this was successful. After the first subtarget, the same procedure has to be completed for the second subtarget on the opposite side and again a beep indicates whether this was successful. The order of reaching those subtargets can be chosen freely. The goal of this procedure is that participants recognize the motion feedback condition, since they are moving from one extreme to the other. For the final part, participants were instructed to slowly approach the center of the main target, indicated by a black dot on white background. As soon as participants reach the center, the third component, the precision hover task, begins. During the 20 s precision hover, a series of beeps is audible to let participants know how long the hover task will last.

We tested three different conditions: no motion (NM), lateral motion (LM), and error motion (EM) feedback. In the no motion condition participants only experienced the live video stream of the octorotor. In the lateral motion feedback, the lateral position and velocity of the octorotor was scaled by 0.4 and reproduced by the CMS. For the error motion feedback we calculated the offset between target and octorotor position and represented this as a roll motion with a scaling factor of 0.2.

Following the definition of motion feedback described in (eq. 4.6) we used $M = 0$ in the no motion conditions. For the lateral motion feedback we defined the elements of M $\alpha_{x_y, x_y^v} = \alpha_{\dot{x}_y, \dot{x}_y^v} = 0.4$, while all other elements were set to zero. This results in the scaling of lateral vehicle position and velocity to lateral position and velocity of the simulator. For the error motion feedback, all elements of M were set to zero except $\alpha_{\eta_\phi, x_y^v} = \alpha_{\dot{\eta}_\phi, \dot{x}_y^v} = -0.2$ and $\beta_{\eta_\phi, x_y^t} = \beta_{\dot{\eta}_\phi, \dot{x}_y^t} = 0.2$.

This results in the mapping of the difference between vehicle lateral position (velocity) and target lateral position (velocity) to simulator roll angle (angular velocity).

For the analysis we calculated the accumulated error for each trial. Accumulated error is defined as the integral of the lateral offset between octorotor and target over time. The smaller the accumulated error the better the operator was able to hover in front of the target.

Every participant completed three sessions, one for each condition. The sessions consisted of 6 trials each and were separated by a break in-between. All participants started with the NM condition first, while the order of conditions for the second and third session were chosen at random.

4.7 Results

Figure 4.3 shows the results of the teleoperation experiment. Figure 4.3a shows the average accumulated error of all participants and their standard deviation for each trial. The accumulated error measurements improve over time, independent of the order of conditions. This is an indication that participants still remained in the training phase resulting in increased variance of the measurements. In a next step we included the effects of training in a statistical model. The red curve shows the fit of how we modeled the training using the equation $f(\text{Trial}) = a \exp\left(-\frac{\text{Trial}}{10}\right) + b$

In Figure 4.3b the average accumulated error of all participants per condition is shown. The white bars show the average accumulated error of all 9 participants. Based on the fit of the model introduced earlier we performed a correction of the measurements to take the effects of training into account. The corrected values are represented by the gray bars in Figure 4.3b. Error bars represent the standard error.

A repeated measures ANCOVA revealed that there is no significant difference between the conditions. However, we found a spike in the accumulated error in the trial that follows when changing the condition from one motion feedback condition to another. In Figure 4.3a the change in conditions is shown by red vertical lines.

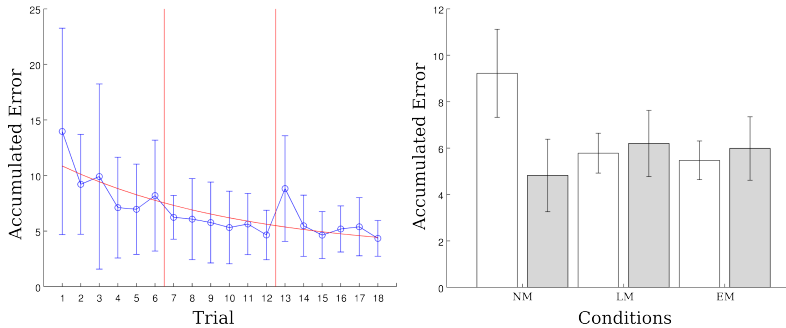

(a) Accumulated error averaged over all participants for each trial (blue). The red curve shows the fitted model of the training. Error bars denote the standard deviation. The vertical red lines mark the switch of conditions.

(b) Average accumulated error for each condition (white), average accumulated error for each condition corrected for effects of training (gray). Error bars denote the standard error.

Figure 4.3: Results and analysis of the accumulated error for 9 participants.

The first change is from condition NM to the first motion feedback condition after trial 6 and the second change from the first to the second motion feedback condition after trial 12. The spike appears for trial 13, which is the first trial after a change in inertial motion feedback condition.

In a second analysis we separated the accumulated error measurements into two groups defined by the order of conditions. In the first group the change of motion feedback condition was from EM to LM, while in the second group the change was in the opposite direction, i.e., LM to EM. The plots in Figure 4.4 show the accumulated error for the two groups for trial 12 and 13.

We found that the spike is independent of the direction of change, it can be seen when changing from linear motion feedback to error feedback or vice versa.

We conducted one-sided paired samples t-tests to compare the accumulated errors of both trials. When changing from the EM to the LM condition we found a significant difference between the two

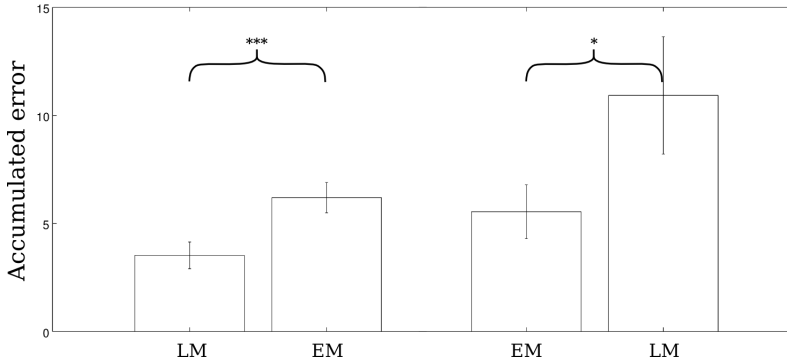

Figure 4.4: Increased accumulated error when changing motion feedback condition. Error bars denote the standard error. The changes are independent of direction of change, i.e. EM→LM or LM→EM.

trials, $t(4) = -2.196, p < 0.05$. When changing from LM to the EM condition we found a significant difference between the two trials, $t(3) = -12.479, p < 0.001$. This signifies that the participants did make use of the motion feedback in their control strategy.

4.8 Formal motion feedback definition and a real-world application

The motion feedback definition introduced in section 4.2 allowed us to describe motion feedback by defining a single motion feedback transformation matrix M. This method uses the freedom granted by the spatial decoupling between operator and vehicle, we were able to shape motion feedback to include task information. Essentially, M allows to describe any linear combination of vehicle state and desired task state.

In addition, we described a teleoperation setup that allows an operator to control an octorotor from a remote location. The teleoperation system is robust and allows for the control of an octorotor over an extended time period. The motion feedback provided to the

operator was defined by the state of the octorotor measured by an optical tracking system. However, systems like this are often not available or feasible, e.g., in vast outdoor environments. In teleoperation scenarios like this, the application of alternative sensors that can determine the position and orientation need to be explored.

The teleoperation setup was successfully used in a teleoperation experiment and we found indications for participants using the motion feedback in their control strategy. The results show a spike in the accumulated error after there was a change in the motion feedback condition. A change in feedback requires a readjustment of the control strategy that incorporates the motion feedback. As this readjustment does not happen instantaneously a temporary increase in accumulated error is the consequence. We argue that if participants use motion feedback to control the vehicle, a strategy is formed on how this additional information can be used. If the type of motion feedback changes, then the strategy used before may not be useful anymore, leading to the increased accumulated error. Since the spike is independent of the direction of change, both types of motion feedback are used in the control strategy of participants.

We were not able to find a significant effect of motion feedback on operator performance. This is unexpected, as the results of the study presented in chapter 2 showed that providing motion feedback in teleoperation had a significant positive effect on the accumulated error. We see multiple reasons that could have produced the results. First, the high variability of the measurements within and between participants had a negative influence on finding a significant difference between conditions. Another reason is that the information contained in the motion feedback depends on the teleoperation task. In the experiment we conducted, the task can be completed purely visually. Although additional feedback channels do increase the overall amount of information, a redundancy in the feedback is present. This may result in the effects of motion feedback being very small. In other teleoperation tasks, e.g., flying an octorotor in a cluttered environment, motion feedback that provides information about the distance to close objects might be beneficial for collision avoidance.

In other studies the effect of additional feedback channels on the operator performance has been investigated, e.g., haptic feedback [Lam et al., 2007]. The focus of this paper was on the possible application of motion feedback in teleoperation, in addition to proposing a method for calculating motion feedback. We see the current results as a promising indication of motion feedback being helpful for the operator. The comparison of motion feedback with other types of feedback channels will be the topic of future research. In addition, although investigating the effects of motion feedback on the mental load and comfort of the operator were not part of this experiment, the potential benefits of reduced workload or increased comfort are important topics for future experiments. We will continue exploring the application of motion feedback in teleoperation scenarios.

Chapter 5
Collision avoidance with motion feedback in teleoperation

5.1 How does motion feedback relate to collision avoidance?

Operators navigating a vehicle through an environment need to process a wealth of stimuli. This is especially challenging in the teleoperation of Unmanned Aerial Vehicles (UAVs), where the operator is controlling the vehicle from a remote ground station. All information needs to be sensed on-board the vehicle and transmitted to the control station, where it is presented to the operator. On-board sensing is limited by the capabilities of the sensors themselves, e.g. noise, update rate, as well as the vehicle, e.g., maximum payload and power supply. In addition, bandwidth limits of the transmission to the control station introduce additional challenges. Transmission delays and noise are common issues in teleoperation that have a negative effect on operating performance [Lane et al., 2002; Sheridan and Ferrell, 1963; van Erp, 2000]. As a result the information available to the teleoperator is limited compared to onboard operation.

Determining the position (interpreting waypoints or maps) of the remote vehicle, estimating the vehicle state (traveling speed, orientation), as well as navigation (obstacle avoidance) heavily rely on vision. The visual system is the most dominant in the information processing of humans [Posner et al., 1976] and can be considered the most important of all human senses involved in teleoperation. Current teleoperation ground stations are usually equipped with

multiple displays that show vehicle state and live video streams captured by one or more onboard cameras [Tvaryanas, 2004].

Position information can be displayed using an overlayed symbol on a map that represents the vehicle position. Other vehicle state information, e.g., orientation, velocity, and acceleration, is usually displayed using visual indicators. These include, but are not limited to, attitude indicator, altimeter, turn and bank indicator, and rate-of-climb indicator. Several different control interfaces are described in [Williams, 2004].

An alternative to providing information about vehicle movements purely visually, is by moving the operator according to the vehicle motion in addition to the visual feedback. In chapter 2 we showed that providing *vehicle-state motion feedback* had a positive effect on operator performance, see also [Lächele et al., 2014]. In this experiment, participants were instructed to hover in front of a series of targets while being subjected to external wind disturbances. In conditions that included motion feedback, the operator perceived the accelerations created by the external disturbances through the motion feedback. This allowed participants to better reject those disturbances, leading to increased hover performance. This is in line with results found in vehicle simulation [Ricard and Parrish, 1984].

However, in teleoperation there is a spatial decoupling between the operator and the remote vehicle. This grants a certain freedom in how motion feedback can be defined, which has the potential to shape motion feedback to include task-related information. In contrast to vehicle-state motion feedback, *task-related motion feedback* does not represent the motion of the remote vehicle. Instead, information about the task is transformed and presented as a motion, which is perceived by the operator. In [Lächele et al., 2016] we investigated the effects of task-related motion feedback on operator performance in a precision hover task. Experimental results showed that task-related motion feedback does indeed improve performance and that motion feedback can be shaped to include task-related information.

The transformation of information contained in one sensory modality (e.g., visual) and presenting it in another modality (e.g., vibro-tactile) is known as *sensory substitution* or *sensory augmentation*.

Initially sensory substitution aimed at replacing a (defective) human sensory modality, e.g., vision, by using information of a (functioning) alternative modality, e.g., tactile [Bach-y-Rita and Kercel, 2003]. Building on sensory substitution, sensory augmentation aims at including additional information to an existing sensory modality. The goal of this approach is to extend the range of what is perceivable by the human. In [Nagel et al., 2005], a vibrating belt is presented that indicates the direction of magnetic north to the wearer. By using a sensory augmentation approach, orientation information that is not directly perceivable by humans (direction of magnetic north) become accessible by extending an existing sensory modality (vibro-tactile sensation). In this sense, task-related motion feedback can be described as sensory augmentation of the vestibular channel with additional task-related information. However, in our work we do not focus on how the human brain interprets the signals or brain plasticity [Bach-y-Rita and Kercel, 2003] involved in the process. Instead, we focus on the application of this approach in a teleoperation setup and the possible benefits for the operator.

In the experiments presented previously, and published in [Lächele et al., 2014, 2016], the teleoperation task was defined as precision hovering in front of one or more targets. Hovering is an important in teleoperation and part of many other control tasks, e.g., take-off, landing, and inspection. However, it is still unknown if and how motion feedback can improve performance in other teleoperation tasks. Therefore, the first research question of this chapter is whether task-related motion feedback improves performance in another common task: collision avoidance. Successfully navigating a remote vehicle in an (unknown) environment depends heavily on avoiding collisions with obstacles. Even minor collisions can lead to costly damages or even a total loss of the vehicle. Therefore, collision avoidance can be considered one of the most important tasks in teleoperation.

Previously, performance benefits of motion feedback could be explained with the operator being able to reject disturbances more effectively. Simulated wind gusts disturbed the motion of the remote vehicle, forcing the operator to constantly correct the vehicle motion to maintain the desired hover position. An explanation for

our findings is that the vestibular system being more efficient in the detection of accelerations than the visual system [Monen and Brenner, 1994; Zaal et al., 2006]. The onset of a wind gust, reproduced by a sudden lateral acceleration, was detected earlier when motion feedback was provided, allowing for a faster correction input. This leads to the second research question. Does vehicle-state motion feedback affect operator performance when the vehicle is not subjected to external disturbances? The answer to this question would provide us with further evidence on the importance of the information contained in the motion feedback. Since the remote vehicle is not subjected to external disturbances, we do not expect a change in operator performance in conditions that include vehicle-state motion feedback.

A common approach to providing collision avoidance feedback is providing haptic feedback [Alaimo et al., 2010; Lam et al., 2007, 2009]. Haptic feedback is achieved by calculating a force, which is proportional to the relative distance and velocity between the vehicle and obstacles in the environment. The resulting force is then presented on the control device and can be perceived by the operator. Providing haptic feedback in teleoperation has multiple benefits. Applying a force on the control input effectively closes the control loop of the remote vehicle. Without the human in the loop, this essentially defines an automated control. The operator has control over how large the influence of the automation is by being more or less compliant with the haptic feedback. Shared control using haptic interfaces has been found to have positive effects on operator performance [Steele and Gillespie, 2001] and visual demand [Griffiths and Gillespie, 2005]. In addition, providing haptic feedback increases the situational awareness in landing remote UAVs [Ruff et al., 2000].

In order to understand the magnitude of the influence of task-related motion feedback on operator performance the results need to be compared to existing solutions that make use of haptic feedback. This comparison between the effects of haptic feedback and the effects of task-related motion feedback is the third research question of this chapter. It is important to provide an objective comparison by calculating the underlying feedback in the same way for the haptic and task-related motion feedback.

To address the research questions we conducted an experiment in which we measured the performance of operators completing collision avoidance tasks while flying along a straight line under different feedback conditions.

The work described in this chapter has been submitted to:

Lächele, J., Pretto, P., Venrooij, J., Zell, A., and Bülthoff, H., "Collision avoidance with motion feedback in teleoperation," *Presence*.

5.2 The teleoperation setup

During the experiment participants were seated in the cabin of the CyberMotion simulator (CMS) (figure 5.1). The CMS is based on an industrial robot[a], mounted on a linear track to improve the linear motion workspace (figure 5.1a). The first rotational axis has been modified to allow for continuous rotation and a custom designed cabin has been mounted at the end-effector of the robot. In total the CMS has 8 axes that can be actuated [Nieuwenhuizen and Bülthoff, 2013].

The cabin of the CMS effectively removes all external influences, e.g. light, wind, sound, that may interfere with the performance of the participants. A projection system projects the view from the simulated on-board camera on a curved screen (120° horizontal field-of-view) inside of the cabin (figure 5.1b).

Depending on the experimental condition the CMS was either not moving, moving in a linear fashion, or rotating around the longitudinal forward axis (roll). A more detailed explanation of the conditions will be given in Section 5.4.

In the experiment, participants controlled a virtual vehicle along a path that is 400 m long, with lateral motion of up to ± 10 m. Movements with such magnitude do not fit into the workspace of the CMS. Therefore, a motion cueing algorithm (MCA) was implemented that maps the motion of the vehicle to simulator motion so that it feels realistic for the operator while preserving physical limits of the motion simulator. We implemented an MCA that is based on a washout

[a] KUKA GmbH, Germany

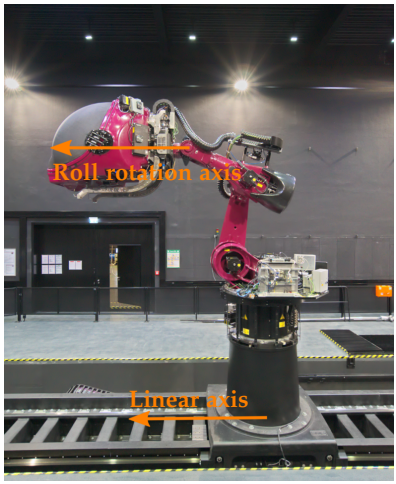

(a) CyberMotion Simulator (CMS) in position to start next experimental trial. The orange arrows show the roll rotation axis and the linear axis.

(b) Cabin of the CMS with cyclic control stick (blue), projection system (green), and the communication headset (red).

Figure 5.1: CyberMotion Simulator with cabin that is shielding participants from unwanted external disturbances (sound, light). Participants can provide control input using the cyclic control stick and can see live video stream that is projected onto the inner curved screen of the cabin door.

filter to provide linear lateral and longitudinal motion. Section 5.4 will go into details of the MCA.

The experiment was conducted using a simulated quadrotor flying in a virtual environment. The simulation environment was implemented using Unity3D[b]. We implemented the dynamics of the quadrotor to resemble the dynamics of a real quadrotor as close as possible. We based the implementation of the quadrotor on previous work [Lächele et al., 2012]. Figure 5.2a shows the visual representation of the quadrotor in simulation.

[b]Unity Technologies, United States

In the experiment participants controlled the longitudinal and lateral position of the quadrotor. Heading and height were controlled automatically and kept constant throughout the experiment. As a result, the motion was restricted to a plane that is parallel to the ground at a height of 1.5 m. The heading was fixed to the direction of forward motion. In all conditions, operators saw a live video feed of a virtual on-board camera that was projected on the inner surface of the CMS cabin. The camera was mounted on a virtual gimbal system that compensated all rotations of the quadrotor resulting in only linear visual motion.

The environment consists of a green ground plane with a straight yellow line drawn on top of it (figure 5.2). Participants were able to start the trial by pressing a button on the control stick that would place the quadrotor at the start position and on top of the yellow line. For the first 10 m gray walls were placed on the left and right side of the line to indicate the direction of flight (figure 5.2b).

While following the line, obstacles in the form of tree trunks would randomly appear on the left or right side. The tree trunks are modeled as vertical cylinders and the position of the trees was defined so that the yellow line would be tangential to the cylindrical body of the trunk (figure 5.2c). The obstacles were defined so that collisions between the quadrotor and the obstacles did not result in quadrotor motion. This was done as a precaution to avoid uncomfortable motion experienced by the operator, upon collision. Instead, to indicate that a collision occurred, the screen turned temporarily red (figure 5.2d).

The radius of the trees was chosen randomly within the interval of 1.5–2 m. Wide obstacles ensured that participants clearly saw where to fly to avoid collisions. In total 10 tracks were created with 14 obstacles each. The distance between two consecutive obstacles was randomly chosen out of a set of distances: $D_l = [20, 23.75, 27.5, 31.25, 35]$. This randomized the distance between the obstacles, ensuring a degree of unpredictability as to when the next collision avoidance maneuver needs to be initiated.

The participants were able to control the remote quadrotor using a cyclic control stick that is located in front of the seat (figure 2.2b). All participants used the right hand to control the vehicle. Only the

(a) Quadrotor passing obstacle in simulation

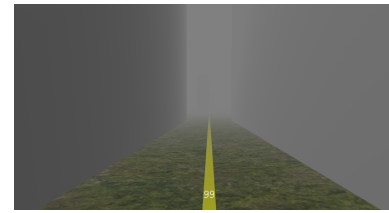

(b) Start of experiment

(c) Simulation as seen by participants

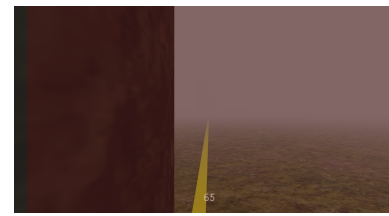

(d) Screen turning red indicating a collision with an obstacle

Figure 5.2: Simulation environment used for the teleoperation experiment. Participants follow a yellow line while being able to move in the longitudinal and lateral directions. Height and heading were fixed throughout the experiment. Simulated fog limited the viewing distance to 9.85 m.

lateral and longitudinal motion could be controlled by moving the stick sideways or forward/backward respectively.

The stick exhibited mass-spring-damper dynamics with self-centering of the stick position, if the operator lets go of the stick. Movements of the stick resulted in a counteracting force consisting of an inertia component (mass), a speed-dependent component (damper) and a position-dependent stick-centering component (spring). With this operators were able to better estimate the magnitude of control input provided.

5.3 Feedback calculation

We calculated the collision avoidance feedback using the Potential Risk Field (PRF) introduced by Lam et al. [Lam et al., 2009]. PRF is a method for calculating a potential field that defines the risk of possible collisions. The PRF consists of two capsules that stretch around the vehicle in the direction of motion. The inner capsule marks an area where a collision with an obstacle inside of it is most likely, the risk is therefore 1. Obstacles outside the outer capsule do not pose a risk of collision and assuming the flight direction of the vehicle does not change, a collision will be impossible. Therefore the risk outside the outer capsule is 0. Between the outer and the inner capsule a gradient defines the risk of having a collision.

Figure 5.3 shows a top-down representation of the vehicle and the surrounding capsules. The vehicle center is depicted with a black and white circle. The grey inner area defines the critical area, obstacles entering this area pose the highest risk of causing a collision. From the critical area to the outer boundary a potential is defined that gradually decreases until the value is 0 at the outer boundary. In addition to extending the field depending on the velocity the outer boundary further extends in the direction of travel by d_{ahead}. This provides the operator with an earlier onset of feedback in the direction of travel..

The radius of the grey critical area is defined by the vehicle radius r_{pz}. The critical area is expanding in the direction of travel by the distance the vehicle needs to come to a full stop, assuming a maximum deceleration $a_{\max}$. Given the vehicle velocity $\boldsymbol{v}$ the inner capsule is therefore extend by $d_{\text{stop}} = \frac{\|\boldsymbol{v}\|^2}{2a_{max}}$. The radius of the outer boundary capsule is the defined by extending the critical area radius by d_{min}. To allow for an earlier feedback onset time (defined by t_{ahead}) in the direction of travel ($\boldsymbol{v}$) the outer boundary is elongated by $d_{ahead} = \boldsymbol{v} * t_{ahead}$.

Based on these two volumes the potential P_{PRF} is calculated in two steps. First, two distances d and d_0 are determined, then the ratio $\frac{d}{d_0}$ is used to calculate the actual response using a potential

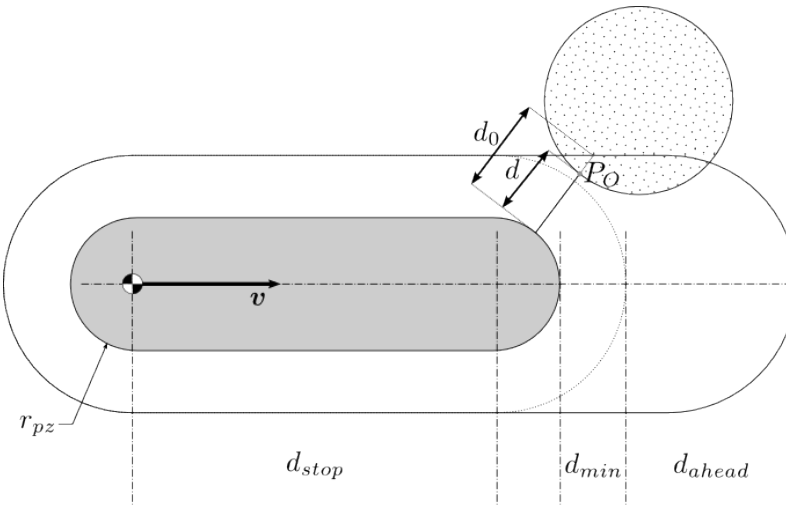

Figure 5.3: Top-down view of the potential risk field (PRF). The grey inner boundary defines the critical area. Obstacles in this area pose the highest risk of causing a collision. Depending on how far an obstacle (dotted circle) reaches between the outer boundary and the critical area ($\frac{d}{d_0}$) a risk of collision is calculated.

function $p\left(\frac{d}{d_0}\right)$. This function can be defined in different ways to ensure certain attributes, like smoothness, of P_{PRF}.

d defines the distance between critical area and *obstacle point* P_O. In this work we used the closest point on the obstacle P_O for our calculations. d_0 defines the distance between critical area and outer boundary (measured through P_O). Therefore, the ratio $\frac{d}{d_0}$ describes how far the obstacle penetrates the potential field. Note that the definition of d and d_0 ensures that $d_0 \geq d$ for all positions of P_O in the potential field. In addition it ensures $d_0 \geq d_{min} \neq 0$, which is important to avoid divisions by zero when calculating the ratio $\frac{d}{d_0}$.

We defined $p\left(\frac{d}{d_0}\right)$ as in eq. 5.1, which ensures two things. First, the results of the calculations of $p\left(\frac{d}{d_0}\right)$ are mapped into the interval $[0, 1]$. Therefore, the magnitude of the feedback that is based on

these calculations will always be within fixed boundaries. Second, the onset of the feedback calculation (P_O at the border of the potential field) has is smooth and has no unexpected jump that could potentially disturb the operator.

$$P_{PRF} = p\left(\frac{d}{d_0}\right) = \cos\left(\frac{d}{d_0}\frac{\pi}{2} + \frac{\pi}{2}\right) + 1 \tag{5.1}$$

In general the potential risk field calculation yields a 3-dimensional vector $P_{PRF} = (P_{PRFx}, P_{PRFy}, P_{PRFz})$. However, in this experiment the remote vehicle is only able to move on a horizontal plane parallel to the ground. The potential field is used to describe an inertial motion feedback and a haptic feedback. Since the obstacles will be approached head-on, feedback information in the longitudinal direction becomes redundant. Therefore, we mapped the 3-dimensional potential field vector (P_{PRF}) to a lateral single value ($\hat{P}_{PRF}$). Eq. 5.2 shows the calculation of $\hat{P}_{PRF}$.

$$\hat{P}_{PRF} = \text{sgn}(P_{PRFy}) \cdot \|P_{PRF}\| \tag{5.2}$$

with $\text{sgn}(x) = \begin{cases} -1 & \text{if } x < 0 \\ 1 & \text{else} \end{cases}$ defined as the sign function, ensuring that the direction of the lateral feedback stays consistent.

5.4 Experiment description

While controlling the remote vehicle, participants were presented with four different types of feedback conditions. In all conditions participants were able to see the environment they were flying in and depending on the condition, we included one of three additional types of feedback. Acting as a baseline for the comparisons we defined a visual feedback only (VIS) condition. In this condition the participant is only able to see the live video stream of an onboard camera.The linear longitudinal and lateral accelerations of the remote vehicle are presented to the operator in the vehicle-state feedback condition (LIN).

The remaining two feedback conditions relied on information about the task, i.e., avoiding obstacles in the environment. The feedback in these conditions was calculated using the potential risk field approach described in 5.3. The core idea of this approach is the definition of a potential that takes the vehicle position and velocity relative to the obstacles into account. As a result, the closer the obstacle and the faster the approach, the larger the potential. This potential value ($\hat{P}_{PRF}$) can then be used to generate a motion or force feedback. In the task-related motion feedback condition (TASK) we rotated the operator around the roll axis depending on the mapped potential field $\hat{P}_{PRF}$. Finally, haptic feedback (HAP) is provided by using the same calculations underlying the TASK feedback, i.e. by scaling $\hat{P}_{PRF}$ and mapping it as a force feedback on the cylic control stick.

Figure 5.2 shows a screenshot of what participants saw during the experiment. A shader was implemented that simulates heavy fog conditions, limiting the viewing distance to 9.85 m. Viewing distance was determined following a similar approach as described in [Pretto et al., 2012]. The luminance of the obstacle ($F_O(x)$) and the background ($F_B(x)$) were measured with a Minolta CS-100 chromameter[c] to calculate the contrast $C_V = \frac{F_B(x)-F(x)}{F_B(x)}$. We then modified the distance between quadrotor and obstacle until we reached $C_V = 0.05$.

This was done so that the next obstacle is only visible shortly after passing the current obstacle. Since the other obstacles are not visible it is not possible for the participant to see the upcoming track and know in advance where the obstacles will appear.

In this condition the operator experiences the linear acceleration of the remote quadrotor. For this we used the scaled linear accelerations of the remote quadrotor as input to a motion cueing algorithm (MCA). We used a filter-based motion cueing algorithm where the vehicle-state accelerations are filtered using a high-pass filter. This is similar to the approach used by classical wash-out filters [Nieuwenhuizen and Bülthoff, 2013]. However, in this work we do not perform tilt-coordination based on low-pass filtering as

[c]Konica Minolta, Tokyo, Japan

would be expected from a classical wash-out filter. The scaling and filtering ensures that the motion simulator does not exceed workspace limitations while returning to an initial position that ensures the agility for subsequent movements.

In eq. 5.3 the transfer function of the high-pass filter to calculate the filtered acceleration $\hat{\boldsymbol{a}}$ is shown.

$$\mathrm{TF}_{HP} = \frac{s^3}{s^3 + 1.3s^2 + 0.5s + 0.075} \tag{5.3}$$

In the next step of the MCA the filtered acceleration $\hat{\boldsymbol{a}}$ is used to calculate a trajectory that is tracked by the CMS. The desired trajectory is defined by a combination of position ($\boldsymbol{p}_d$) and velocity ($\boldsymbol{v}_d$) of the simulator cabin, obtained by integrating $\hat{\boldsymbol{a}}$. In the last step, the trajectory is used as input for an inverse kinematic controller of the CMS that tracks this trajectory. More on the specifics of the CMS motion cueing algorithm and the inverse kinematic controller can be found in [Giordano et al., 2010a,b; Nieuwenhuizen and Bülthoff, 2013].

In TASK motion feedback conditions the cabin was rolled according to the potential risk field ($\hat{P}_{PRF}$) value. The larger $\hat{P}_{PRF}$, the larger the rotation towards the obstacle. This behavior emulates an acceleration of the quadrotor in the direction of rotation. Since this was not commanded by the operator, it would represent a disturbance that needs to be counteracted by providing an input in the opposite direction, i.e., moving the control stick away from the incoming obstacle. As a result the operator initiates an avoidance maneuver.

The scaling of the feedback determines when the resulting motion can be perceived by the operator. In addition, larger feedback early in the approach of the obstacle results in a larger reaction, i.e., control input, by the operator. When testing the experimental conditions, we determined that a scaling factor of 0.15 would provide recognizable feedback early in the approach. At the same time the roll motion did not exceed $\pm 8.59°$ ensuring that participants are not disturbed by large roll rotations.

The haptic feedback was defined by scaling the P_{PRF} value and applying a force in the opposite direction of the obstacle. This way,

being perfectly compliant with the haptic feedback would lead to an avoidance maneuver around the obstacle with no collision. However, this avoidance maneuver would not necessarily be optimal, since the distance to the obstacle would be larger than necessary. On the other hand, reducing the scaling would reduce the strength of the haptic feedback, with the effect of participants perceiving the feedback at a later point in time, reducing the effectiveness of the haptic feedback. Participants were instructed to find a balance between being compliant and flying an optimal path around the obstacles in the training trials.

In summary, the haptic feedback was calculated with $F_{\text{haptic}} = \hat{P}_{PRF} * F_{\max}$, with $F_{\max} = 35\,\text{N}$ During the development of the experiment, care was taken that operators are always able to counteract the forces of the stick. This is important to ensure that operators are always in command of the vehicle.

The main goal of this work is to investigate how motion feedback can benefit the operator in a teleoperation collision avoidance task. The task description of this experiment states that participants had to complete the task as fast and as safe as possible. Therefore, we used the *number of collisions* (N_{col}) and the *trial completion time* (Δt) as measure of the performance of the operator. If participants are able to complete trials faster with less collisions, the task performance is larger than trials with larger completion time or more collisions.

However, number of collisions and completion time do not completely describe the behavior of participants and potential changes induced by the experimental manipulations. For this we introduced two additional measures, the *avoidance maneuver onset time* (t_{onset}) and the *minimum passing distance* (D_{min}). The avoidance maneuver onset time describes how many seconds before reaching the oncoming obstacle participants started with the avoidance maneuver. The minimum passing distance is calculated by determining the minimum distance between the vehicle and the obstacle while the vehicle is passing it.

Figure 5.4 shows examples for t_{onset} and D_{min}. The avoidance onset time is defined by the input given by the operator. Flying around an obstacle requires the operator to provide stick input. At

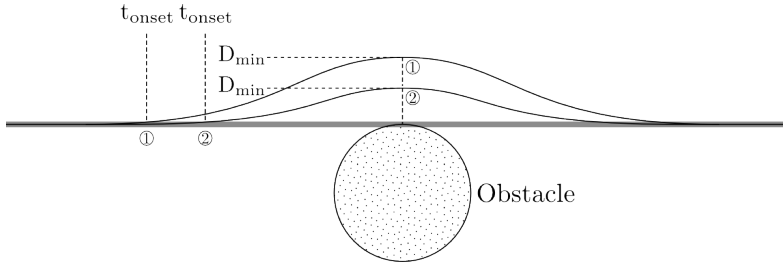

Figure 5.4: Two exemplary avoidance maneuvers with avoidance maneuver onset time t_{onset} and minimum passing distance D_{min} shown. In scenario ①, the operator starts avoiding the target earlier and a larger minimum distance to the obstacle (D_{min}) is maintained. The risk of a collision is reduced, hence the operator flies safer. In scenario ② a more risk-taking flight is shown with a late avoidance onset and smaller minimum passing distance.

some point before the obstacle this input will reach a maximum. However, this point does not accurately describe when the avoidance maneuver started, since time is needed to reach this maximum. We therefore consider the velocity of the stick movements before reaching maximum stick deflection. From the dynamics of the stick follows that at some point before reaching the stick deflection maximum, the stick deflection velocity also reaches a maximum. We determine this point in time and use this as the estimate of the onset of the avoidance maneuver. Using this approach we can more accurately calculate the duration between avoidance maneuver onset and passing of the obstacle.

Finally, we calculated the overall stick deflection during the trial to estimate the effort participants had to invest in controlling the quadrotor. Stick deflection was defined as the root mean square of the *lateral stick deflection* (RMS_α) as described in eq. 5.4.

$$RMS_\alpha = \sqrt{\sum_{i=1}^{n} \frac{1}{n} \alpha_i^2} \tag{5.4}$$

Where α describes the stick deflection in radians and n the number of samples for the trial. This is equivalent to calculating the standard

deviation of a discrete random variable with zero mean ($\mu = 0$) where all events are equally likely. This is taking the same approach as in [Venrooij et al., 2014] and is similar to what can be found in literature where the variance [Nieuwenhuizen et al., 2011] or the standard deviation [Lam et al., 2007] is used as a measure for control effort or control activity. A benefit of this measure is that smaller inputs, attributed to corrective inputs, are influencing the measure less than large inputs, attributed to intentional flight direction changes. This effectively filters out small corrective inputs and allows to focus on the main control input given by participants.

To summarize, by using the number of collisions and the completion time we gain insights into the performance. In addition, we can describe how the behavior of the operator relates to safety by analyzing the avoidance onset time and minimum passing distance. Since different conditions may affect control effort differently, we also use the Control effort RMS_α measure to analyze those changes.

Participants were instructed to control a remote quadrotor and fly along a yellow straight line on the ground. The goal was to fly as fast as possible while trying to avoid collisions with randomly appearing obstacles and staying as close as possible to the yellow line. Trees would appear tangentially either on the left or the right side of the yellow line. Ten different tracks were generated, containing each 14 obstacles. The order of conditions was chosen randomly. This removed learning effects from the averaged data and ensured that participants were not able to recognize a track and remember the positions of the obstacles. Participants then completed a block of 10 trials with the same condition before moving on to the next condition. After completing a block of 10 trials, participants were notified that there will be a change in condition, but the next condition was unknown. After 20 trials participants had a 15 min break, before completing the last 20 trials. On average the total experiment duration was 110 min, which includes the initial task explanation, training time, and between-trial breaks.

At the beginning of the experiment participants completed 20 training trials where the order of conditions was not random. The first condition was always the VIS condition (5 trials) followed by the haptic feedback HAP condition (5 trials). In both of those

conditions there was no inertial motion feedback provided and participants were able to familiarize themselves with the control task. Then, participants completed 5 trials with the vehicle-state motion feedback (Lin-On) and finally 5 trials with the task-related motion feedback (Task-On). After the training we included a 15 min break, where participants left the simulator before starting the first block of 20 trials.

The task instructions do not define which strategy participants should use in completing the task. For example, a cautious participant could fly slow in order to always have enough time to avoid the next obstacle. A more risk-taking participant could focus on completing the task as fast as possible, with less emphasis on avoiding collisions.

To ensure participants fly as fast as possible, while avoiding collisions, and as close as possible to the straight yellow line, we implemented a score system based on points. For each trial participants started with 100 points. For the duration of each trial points were subtracted depending on the number of collisions, the offset of the quadrotor from the center line, and the time spent in the trial. The points were displayed in the lower center of the screen and participants were able to see their current points throughout the trial (see digits in figure 5.2c).

This approach lead to participants trying to keep as many points as possible, while finding a balance between reducing the number of collisions, flying close to the reference line, and flying fast, according to the experimental conditions.

Eq. 5.5 shows the calculation underlying the points score system that depends on the number of collisions, lateral offset, and the time to complete a trial. In the training phase of the experiment each participant was instructed to provoke collisions and deviate from the center line to get an understanding of how collisions or large lateral offsets affect the points. This also showed participants that collisions with obstacles do not affect the motion of the simulator.

$$p_{\text{end}} = 100 - \underbrace{N_{\text{col}} \cdot 25}_{\text{collision penalty}} - \underbrace{\int_0^{\Delta t} \mathbf{x}_y^2 \, \mathrm{d}t}_{\text{off-center penalty}} - \underbrace{0.5\Delta t}_{\text{time penalty}} \tag{5.5}$$

where Δt is the completion time, N_{col} the number of collisions, and $\mathbf{x}_y$ defines the lateral position offset between the quadrotor and the yellow straight line.

This score system combines several measures into one with the goal of directing participants towards a common flight strategy. From the point score it is impossible to infer differences between the conditions, since multiple measures are combined. Therefore, the points will not be included in the analysis of the results. However, the analysis will focus on the components, i.e., collisions, off-center distance, and completion time, that make up the score.

In total 17 naïve participants (5 females), i.e., participants did not have extended experience in the teleoperation of quadrotors, took part in this study after signing a consent form. This form briefed participants that participation is voluntary and can be cancelled at any time. Due to mild symptoms of motion sickness in the training phase 4 participants aborted the experiment. For the analysis the data of the remaining 13 participants (5 females) were used. All participants had normal or corrected-to-normal vision.

5.5 Results

In the following, results are reported for the measures of performance, behavior, and control effort respectively. We used one-way ANOVAs to test the statistical significance of differences in the measurements, with participant defined as a random factor. This is mathematically equivalent to a repeated-measures ANOVA. For the post hoc comparisons of means, we used Bonferroni corrections.

Performance

The average number of collisions per trial and condition was 0.71, with no significant differences among conditions (figure 5.5a). This is

a surprising results, since we expected a reduction in the number of collisions for feedback conditions that include obstacle information, i.e., TASK and HAP.

Instead, we found a statistically significant main effect for completion time between conditions as determined by a one-way ANOVA ($F(3, 504) = 67.67, p < 0.0001$). Post hoc tests with Bonferroni correction for multiple comparisons revealed a statistically significant reduction in completion time for the TASK and HAP conditions, when compared to VIS and LIN (figure 5.5b). We also found that the completion time is significantly lower in HAP compared to the TASK condition. Moreover, no statistically significant difference between the VIS and LIN conditions was found.

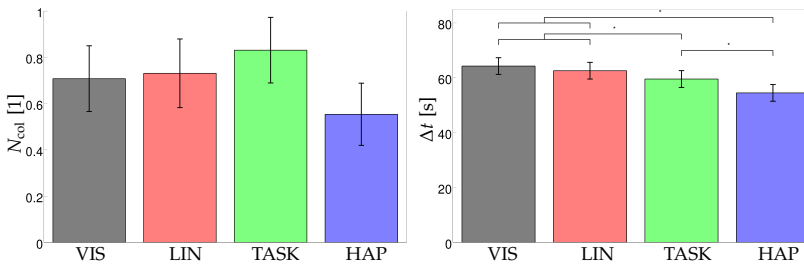

(a) Number of collisions (b) Completion time

Figure 5.5: Number of collisions and completion time averaged over all trials and participants. Error bars denote the standard error.

Behavior: avoidance maneuver onset time and minimum passing distance

Starting from the central yellow line, participants had to initiate avoidance maneuvers around upcoming obstacles. The closer the distance to the obstacle the higher the risk of colliding with the obstacle. The avoidance onset time (t_{onset}) and minimum passing distance (D_{min}) give insight into how safe the flight behavior of a participant is. Increased onset times and larger D_{min} show safer flight behavior, i.e., reduced risk of collisions.

Figure 5.6a shows the results of avoidance onset time (t_{onset}). We found a significant main effect ($F(3, 504) = 55.04, p < 0.0001$) for t_{onset}, being significantly larger in the TASK and HAP conditions compared to the VIS and LIN conditions. In addition we found a significant difference between the TASK and HAP condition, i.e., t_{onset} is larger in the HAP condition compared to TASK. These results are in line with the hypothesis that participants start the avoidance maneuver at an earlier point in time, when task-related feedback is provided, indicators for a safer flight behavior.

This shows that participants initiate the avoidance maneuver earlier in conditions that include obstacle information, i.e. task-related motion feedback (TASK) and haptic feedback (HAP), compared to the visual feedback (VIS) and vehicle state-related (LIN) feedback and that participants are able to use the task-related information included in the feedback.

Figure 5.6b shows the average minimum passing distance D_{min}. We found a significant main effect ($F(3, 504) = 90.17, p < 0.0001$) with D_{min} increased in conditions that included obstacle information (TASK, HAP) compared to conditions that did not (VIS, LIN). That means that in both the VIS and LIN conditions participants were taking higher risks, i.e., passing closer to the obstacles, compared to the other two conditions that included additional feedback about the obstacle.

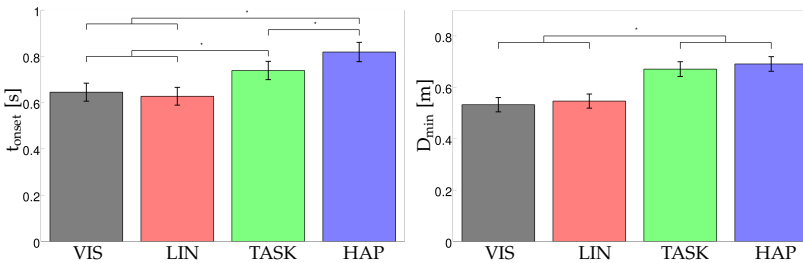

(a) Average avoidance onset time per condition

(b) Average minimum passing distance per condition

Figure 5.6: Avoidance onset time (t_{onset}) and minimum passing distance (D_{min}) averaged over trials and participants. Error bars denote the standard error.

Control effort (RMS_α)

Figure 5.7 shows the average control effort per condition. We found that in the HAP condition the stick deflection (RMS_α) is significantly smaller compared to the other conditions, which do not differ from each other ($F(3, 504) = 63.69, p < 0.0001$). This means that participants on average had to invest significantly less control effort in the HAP condition.

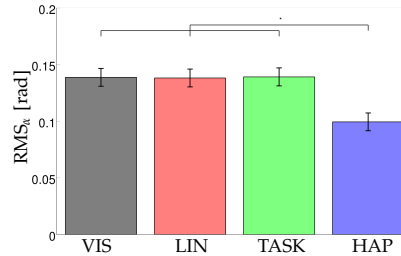

Figure 5.7: Average control effort of all trials and participants, defined as stick deflection (RMS_α). Error bars denote the standard error.

5.6 Task-related feedback in teleoperation collision avoidance

Participants were instructed to fly as fast and as safe as possible along a straight line on the ground. Depending on the condition, additional feedback about the vehicle or the obstacles in the environment was provided.

The results show that providing task-related motion feedback (TASK) in addition to visual information does not affect the number of collisions. In fact, the number of collisions does not differ significantly across conditions.

However, we found that task-related motion feedback (TASK) and haptic feedback (HAP) reduce completion time. This is interesting, because it shows that participants use feedback to increase flight speed rather than reduce the number of collisions. We used

a points score system to help participants follow the instructions of the task. Although the loss of points due to a collision can not be recovered by increased flight speed, participants still chose a strategy to fly as fast as possible.

In addition, we found that participants started the avoidance maneuver at an earlier point in time in those conditions. This shows that obstacle information is available at an earlier point in time compared to the VIS and LIN conditions. We found that on average participants use this information to fly faster, leading to a reduced completion time. This additional information is also used to change flight behavior by keeping a larger distance to obstacles, i.e., increased D_{min} in TASK and HAP conditions. These are signs of a safer flight, however, this is not reflected in the number of collisions. To summarize, participants are able to fly faster while maintaining safer distances to obstacles in conditions that include task-related information.

An alternative explanation is that the increase in minimum passing distance is a direct result of the increased flight speed. With fast movements even small directional changes lead to an increased offset and in turn to increased D_{min}. If that would be true, we would expect a larger control activity (RMS_α) in order to return to the center line. However, we do not find increased RMS_α in conditions that also show increased flight speeds, i.e., TASK and HAP. In fact, we found no difference between the conditions, with the exception of decreased RMS_α in the HAP condition. Therefore, it is plausible to reject the hypothesis that increased D_{min} is solely caused by increased flight speed.

We found no significant effects of vehicle-state feedback (LIN) on any of the measurements. It can be concluded that the additional vehicle-state information does not contribute to completing the task better. Previous experiments suggest that vehicle-state feedback improves operator performance due to increased disturbance rejection capabilities [Lächele et al., 2016]. In this experiment we did not simulate any external disturbances, therefore changes in performance in the LIN condition were not expected. The results of this experiment provide additional evidence for the hypothesis that vehicle-state

feedback is useful in tasks that require information about external disturbances.

Overall we found the TASK condition to be significantly different to the HAP condition in this experiment. Although we see improvements in the TASK condition, the improvements are always smaller than in HAP conditions. In an informal debrief after the experiment, we asked participants, whether the TASK feedback was perceived to be intuitive. Only three participants out of 13 considered it to be intuitive. This could indicate that participants had to spend additional mental effort to understand the meaning of the additional feedback during the flight.

This may be a result of the sensory augmentation approach we used to define the TASK condition. In the TASK condition, a rotation is perceived, which needs to be interpreted before an understanding of the obstacle location in the environment can be formed. This requires additional time, explaining the differences between the TASK and HAP condition we found in the results.

In our experiment training consisted of completing 20 trials, which took around 30 min. In comparison, participants of a sensory substitution study conducted by Nagel et al. [Nagel et al., 2005], trained the usage of a sensory augmentation device (vibrating belt) over a period of several weeks to ensure that no high-level cognitive reasoning is required. It stands to reason that the cognitive load needed to interpret the task-related motion feedback would decrease given more training time.

Likely, in the HAP condition less mental processing is required to understand the meaning of the feedback. The level of being compliant with the feedback of the stick, i.e., the stiffness in holding the control stick, controls how the feedback is used in the avoidance maneuver. Changes in the stiffness result in increased or reduced compliancy and in turn in increased or reduced avoidance onset time (t_{onset}) and minimum passing distance (D_{min}).

Increased compliance with the control stick is also reflected in the control activity of this experiment. The control activity (RMS_{α}) is reduced only in the HAP condition, no other significant differences were found between the other conditions. The results show that in the HAP condition participants were able to provide smooth control

input with less changes in the deflection. We see this as a result of participants using the haptic feedback by adjusting compliancy, leading to less corrections and a reduced RMSα.

The Potential Risk Field (PRF) used in the task-related and the haptic feedback depends on the current velocity of the vehicle. Since participants are able to use the feedback to increase the average flight speed, the capsules extend further than the distance of visual obstacle detection. This results in an earlier detection of the next obstacle compared to the VIS and LIN conditions where the next obstacle can only be detected visually.

In this experiment we made a distinction between two types of motion feedback, either task-related or vehicle-state feedback. We did not include a condition where the motion provided is a combination of both. It would be interesting to investigate whether this is the reason why the majority of participants found task-related motion feedback to be less intuitive. A future experiment could implement a condition where the full spectrum of quadrotor motion is provided, i.e. roll, pitch rotations, linear accelerations, in combination with additional task-related motion, e.g., additional rotations proportional to the distance to obstacles.

In this Chapter we focused on three research questions. Can task-related motion feedback increase performance in a collision avoidance task compared to visual only feedback? Does vehicle state-related motion feedback affect performance in the absence of external disturbances? And finally, how does task-related motion feedback compare with providing haptic feedback, a common approach in collision avoidance tasks? To answer those questions we conducted an experiment where we measured the performance, i.e., number of collisions (N_{col}) and completion time (t_Δ), behavioral changes, i.e., avoidance onset time (t_{onset}) and minimum passing distance (D_{min}), and overall stick deflection RMS_α.

The results of the study presented in this chapter show that the number of collisions is independent of the feedback condition. Participants are able to fly faster while maintaining safer distances to obstacles in conditions that include task-related information. However, we found significant differences between the task-related motion feedback (TASK) and haptic feedback (HAP) conditions, with

haptic feedback being superior in terms of completion time (t_Δ) and evasion onset time (t_{onset}). Furthermore, we found a significant reduction of control effort (RMS_α) only in the haptic feedback (HAP) condition. We also found that vehicle-state feedback (LIN) did not affect any of the measures in this experiment. This can be considered a clear indication that this type of motion feedback improves performance in disturbance rejection tasks only. This is in line with previous results, where it was suggested that vehicle-state feedback increases disturbance rejection capabilities of operators.

Haptic and motion feedback are not mutually exclusive and can be presented simultaneously. A future experiment could investigate how providing both types of feedback simultaneously affects operator performance in teleoperation. In this future experiment the information contained in the feedback would differ to avoid redundancy. Haptic feedback could provide information about obstacles in the environment, while task-related motion feedback could provide feedback about a secondary task, e.g., tracking a predefined trajectory. This could enable operators to better control remote vehicles without the need for additional visual displays. In fact, a setup like this could potentially allow for operators to complete the task even in extremely poor visual conditions.

Chapter 6
Discussion

The goal of this thesis was to investigate the effects of providing motion feedback to the operator in a teleoperation setup. The hypothesis was that providing motion feedback has positive effects on operator performance, based on the results of previous research [Robuffo Giordano et al., 2010].

In Chapter 2 a first teleoperation experiment is presented, where participants were instructed to perform a series of hover tasks. The results show that participants were able to improve performance, i.e., in conditions with motion feedback the precision in staying in front of the target was increased. Furthermore, the results show that participants significantly increased their control activity in conditions with motion feedback, indicating increased control effort.

These results are in line with existing work, where operators were given the task to control a vehicle, while the vehicle was subjected to external disturbances [Pool et al., 2008; Ricard and Parrish, 1984; Scanlon, 1987; Zaal et al., 2009]. In those studies participants were presented with the accelerations of the vehicle using a motion simulator. The results show that participants were able to improve performance. This was explained with participants being able to perceive accelerations caused by disturbances faster. This lead to participants providing faster and larger corrective input, which in turn reduced tracking errors. The studies found that participants had to invest more control effort in conditions that include motion feedback, supporting this explanation.

A detailed analysis of the results described in chapter 2 further confirmed this explanation. The wind disturbances introduced in the experiment acted only on the lateral motion of the quadrotor, while

vertical motion was not affected by wind. It was found that tracking precision was improved only in the lateral direction of motion. In addition, control activity was increased only in the direction that controlled lateral motion.

This showed that motion feedback can increase performance in teleoperation hover tasks. It also provided additional evidence that increased performance is due to increased disturbance rejection capabilities. However, in the experiment lateral motion consisted of a roll rotation and an acceleration in the direction of roll. The experimental design did not allow to make conclusions as to how the performance is related to these individual components of motion (roll rotation and lateral translation).

Chapter 3 presents the results of two experiments. In the first experiment, the goal was to identify the contribution of the rotational and linear components of vehicle-related motion feedback on control performance. The second experiment tested the hypothesis that the spatial decoupling between the operator and vehicle – typical of teleoperation – introduces the possibility of shaping motion feedback. This could lead to the possibility of optimizing motion feedback with the goal of maximizing operator performance. For this, knowledge about the contribution of different motion feedback components on operator performance is essential before adjustments can be made.

In the experiments described in chapter 3, participants controlled a remote vehicle from within the cabin of a motion simulator while the virtual quadrotor was flying in a simulated environment. Similar to the experiment in chapter 2, participants were given a precision hover task while the quadrotor is being subjected to wind disturbances. While performing the hover task, lateral wind gusts acted on the frame causing the operator to constantly provide corrective input to stay on target.

The results showed operator performance was increased only in conditions that included lateral motion feedback. The roll motion component did not affect performance, however, a reduction in stick activity was found. Additional information about the disturbances was only available in lateral motion feedback conditions, since wind acted only on the linear motion of the quadrotor. This

lead to increased disturbance rejection capabilities and increased performance.

The fact that roll motion did not provide additional information and did not contribute to performance was used in the second experiment described in chapter 3. The same experimental design, i.e., control task, environment, procedure, was used in this second experiment. However, the condition that included vehicle-related roll motion feedback was exchanged by a roll motion feedback condition that represented the offset between target and vehicle position. This new type of motion feedback, called task-related motion feedback, did not represent the motion of the vehicle. Instead, it provided feedback about the task itself; the larger the offset between quadrotor and target the larger the roll rotation. The goal of the second experiment was to show whether task-related motion feedback can improve operator performance. Indeed, the results showed a improved performance in task-related motion feedback conditions.

Task-related motion feedback exploits the spatial decoupling typical of teleoperation. This changes the role of providing motion feedback usually found in vehicle simulation. In vehicle simulation the intention of providing motion feedback is to increase the realism of the simulation, while in teleoperation it has the potential to be used as a tool for providing additional feedback about the task. This feedback would not be available in a teleoperation setup that aimes at reproducing vehicle-state information only. This approach is inspired by the research on sensory substitution and augmentation and introduces a wide range of possibilities for the design of operator control stations.

Sensory substitution describes the process of transformation the information and characteristics of one sensory modality to another. The motivation of sensory substitution is the replacement of a defective sensory modality by another. One application is the support of the blind by providing vibro-tactile feedback about surrounding obstacles or points of interest [Bach-y-Rita and Kercel, 2003]. Sensory augmentation describes the extension of a sensory modality with information of another, rather than replacing it. A common approach found in sensory augmentation is providing vibro-tactile

or haptic feedback that is based on information provided by various sensors [Loomis et al., 1993; Petzold et al., 2004; Wu et al., 2015].

Similarily, task-related motion feedback describes a sensory augmentation process where visual information (e.g., offset to a target) is transformed and mapped to motion (e.g., roll rotation). The work presented in chapter 3 showed that sensory augmentation can be used in teleoperation with positive effects on operator performance.

However, at this point the effectiveness of task-related motion feedback has been shown for a single task only. Furthermore, the teleoperation experiment was conducted in a simulated environment. Before further exploring possible applications of task-related motion feedback it was important to validate the feasibility of the approach in a real world scenario. Here, feasibility refers to the technical challenges of providing motion feedback in a real teleoperation setup.

Chapter 4 shows a teleoperation setup where the operator controls a real octorotor. The experiment described in chapter 4 was based on the design described earlier in chapter 3. Again, the task was to hover in front of a target as precise as possible, while the operator perceives different types of motion feedback. The experimental conditions included a visual feedback only condition, vehicle-related roll and linear motion conditions, and a task-related motion feedback condition. The goal of the experiment was to determine the feasibility of the approach, i.e., what the technical challenges of implementing such a system are.

The system was successfully implemented and used in a teleoperation experiment. In addition a method for calculating motion feedback was described. First, the state of the vehicle and the desired state were described as time-varying vectors. Using a matrix multiplication any linear combination between the vehicle state and the desired state can be described.

Although the same conditions were used as in the previous experiments described in chapter 3, we were not able to find the same effects, i.e., we were not able to find significant differences between conditions that included additional motion feedback and conditions that did not.

However, results indicate that participants use motion feedback when controlling the octorotor. A sudden increase in the hover error was found when a switch from vehicle-related to task-related motion feedback occured and vice versa.

Several technical challenges remain in the teleoperation setup. Different communication channels exist that introduce different time delays into the system. This could be an explaination of why no difference between the conditions was found. Perceiving motion that is not exactly correlated with the visual motion might act as a disturbance to the operator. However, the results are not conclusive and future experiments could focus on varying the time delay of the individual feedback channels to determine possible effects on operator behavior and performance.

The system described in chapter 4 shares similarities to other teleoperation setups found in literature. In [Robuffo Giordano et al., 2010], participants controlled a remote quadrotor while perceiving different types of motion feedback. The task was to fly from a start position to a target position and remain there as precise as possible. In halve the conditions participants controlled either a virtual quadrotor in a simulated environment or a real quadrotor.

Results of that study showed no significant differences between conditions in the case of controlling a real quadrotor. This is in line with the findings presented in chapter 4. However, when controlling a simulated quadrotor, Robuffo Giordano et al. found that performance was decreased in motion feedback conditions. This is contrary to the results of chapter 2 and chapter 3, where a significant performance improvement was found for both vehicle-related and task-related motion feedback.

A possible explanation for this could be the difference in how lateral linear motion is provided between the setup of Robuffo Giordano et al. and the setups presented here. In [Robuffo Giordano et al., 2010] the motion cueing algorithm maps lateral motion to a cylindrical motion of the cabin. This was done to extend the lateral motion envelope of the motion simulator. However, this introduces additonal rotational cues that could potentially disturbe the operator. In the experimental setup presented here, this was not an issue, because the simulator was mounted on a linear track

that increased the linear motion space significantly. This way lateral motion could be reproduced without introducing false motion cues.

Teleoperated quadrotors can be used in a plethora of tasks, but some tasks are required more often than others. Hovering, i.e., maintaining a position and a certain height, can be considered the most common task, since it is often a subtask, e.g., take-off and landing. Due to their hovering abilities, quadrotors are often used in “eye-in-the-sky" operations, e.g., aerial inspection or search and rescue. Due to its importance in teleoepration, the experiments presented so far focused on hovering tasks.

Another important task in teleoperation is avoiding collisions with objects in the environment. Even small collisions can result in the loss of the vehicle along with the (expensive) equipment onboard of it. In chapter 5 a teleoperation experiment is presented with the goal of determining wheter task-related motion feedback can improve performance in a collision avoidance task.

The second goal of the experiment is to provide a comparison to haptic feedback. Providing haptic feedback is commonly found in vehicle operation with positive effects on performance and control effort [Alaimo et al., 2010; Griffiths and Gillespie, 2005]. In [Lam et al., 2007, 2009] haptic feedback proofed to be successfull in the teleoperation of a remote helicopter in a collision avoidance task. Therefore, the experiment included a condition where haptic collision avoidance feedback was provided. The calculations underlying the collision avoidance feedback were the same for both the haptic and the task-related motion feedback. For this a Potential Risk Field (PRF) was defined that calculates the risk of collision with obstacles in the vicinity of the vehicle [Lam et al., 2007]. The larger the risk, the larger the feedback presented to the operator.

Results of this study show that the number of collisions is independent of the feedback condition. This is unexpected since other research shows that the number of collisions is reduced when haptic feedback is provided. Instead, we found that participants fly faster while maintaining safer distances to obstacles in conditions that include task-related information. This shows that task-related motion feedback can improve the behavior of participants in collision avoidance tasks.

However, when comparing the effects with haptic feedback we found that the effects of haptic feeedback are superior in terms of completion time and evasion onset time. Furthermore, we found a significant reduction of control effort only in the haptic feedback condition. Providing vehicle-state linear motion feedback did not affect any measures in the experiment. With the absence of external disturbances no effects can be expected when providing vehicle-state motion feedback. This is in line with previous results shown in chapter 2 and chapter 3.

The results of the experiment showed that the effects of task-related motion feedback on the behavior are comparable with the effects of haptic feedback. What was also shown is that not all types of motion feedback are helpful for the operator. In conditions that included vehicle-related linear motion feedback the performance, behavior, and control effort remained unchanged compared to the baseline condition, where only visual feedback was provided. This is interesting, since it further supports the notion that motion feedback needs to include additional information about the task for the operator in order to improve performance or behavior. Linear motion feedback did not include task-related information, since no external wind disturbances were present and no information about the obstacles was included. However, haptic and task-related information did include information about the obstacles, which lead to improved performance.

This thesis shows the effectiveness of motion feedback in teleoperation. In order to improve performance the motion feedback needs to include task-related information for the operator. This was shown in tasks where information about wind disturbance was included in vehicle-state motion feedback. In addition, the spatial decoupling between operator and vehicle allowed for the shaping of task-related motion feedback, which is unique to teleoperation. Presenting task-related motion feedback proofed to be helpful for hovering and collision avoidance tasks.

This thesis does not answer the question how the motion feedback should be shaped depending on the task or the vehicle. Rules for how the mapping of task-related information to a motion feedback has to be defined can not be derived from the results presented

here. It is highly suggested to focus future research on this topic, based on the positive results of this thesis and the vast possibilities this method introduces for the shaping of motion feedback and possible benefits for teleoperation.

Knowing how to best define task-related motion feedback given the task is an important step towards being able to provide optimal motion feedback. Motion feedback is optimal when performance is significantly increased and no other type of motion feedback would further increase performance. Another step to providing optimal motion feedback is knowing the relationship to other types of feedback. It is important to know how motion feedback interacts with other types of feedback, e.g., haptic, tactile, or auditory. Depending on what types of feedbacks are presented the benefits of providing motion feedback could change. This could also be dependent on the workload of the operator.

Future experiments could focus on these topics with the goal of defining optimal motion feedback that significantly increases operating performance and safety in the teleoperation of UAVs.

Chapter 7
Conclusions

The goal of this thesis was to investigate how motion feedback can be beneficial in the teleoperation of Unmanned Aerial Vehicles (UAVs). The hypothesis was that by providing additional motion feedback the operator has more information available, resulting in improved operator performance. Two types of motion feedback were introduced, vehicle-related and task-related motion feedback. Vehicle-related motion feedback presents the operator with the motion of the remote vehicle. Task-related motion feedback is a combination of the vehicle state and the desired state that is defined by the task at hand. This type of feedback therefore includes additional information about the task. Presenting task-related motion feedback exploits the defining feature of teleoperation, spatial decoupling of the operator and the vehicle.

The results of the first experiment described in chapter 2 show that motion feedback improves performance in teleoperation. The task was to hover as precisely as possible in front of a series of targets. Participants could control thrust and the lateral position using collective and cyclic control sticks. While completing the task external wind disturbances acted on the quadrotor body, forcing participants to constantly provide corrective input.

The wind gusts only acted on the lateral and not on the vertical motion of the quadrotor. The performance analysis was performed for the lateral and the vertical component individually. This showed that significant performance improvements were only found in the lateral component of motion. Participants were able to perceive the motion of the quadrotor and the external disturbances in motion feedback conditions leading to better performance in rejecting the

wind disturbances. This is in line with the results of Hosmann, Pool et al., and Zaal et al. [Hosman, 1996; Pool et al., 2008; Zaal et al., 2009]. Their findings are explained by the vestibular information being processed faster, compared to visual information, which then leads to increased control performance. An increase in stick deflection of the cyclic stick, which is used for controlling lateral motion, was found. Participants performed larger and faster stick deflections in conditions that included motion feedback. This further strengthens the explanation of increased disturbance rejection capabilities of tele-operators due to motion feedback.

The results of the first experiment show that motion feedback can be beneficial for teleoepration tasks. But the results do not allow for identifying the source. Lateral motion of the quadrotor always consists of two components, lateral linear motion and roll rotation. The operator was therefore always presented with both components simultanously, making it impossible to identify the contributions of the individual components to the improved performance.

Identifying these contributions was one goal of the experiments described in chapter 3. For this the individual components (roll rotation and lateral translation) were presented to the operator, which allowed to determine their contribution on operator performance. This is a first example of how the spatial decoupling can be used to modify the motion of the vehicle before it is presented to the operator. The concept of modifying motion feedback is extended by defining task-related motion feedback. In a second experiment the effects of this novel motion feedback was studied. First, the offset between desired position in front of the target and the actual vehicle position is calculated. In a second step this offset is scaled and mapped to a roll motion. This roll motion does not represent the motion of the vehicle but instead provides feedback about the task. This allows to reformulate the goal of the teleoperation task. Instead of hovering in front of the target as precise as possible, the task can be completed by staying as upright as possible.

The results presented in chapter 3 show that the linear lateral motion was the single contributing factor for increased performance. Vehicle-related roll motion did not affect performance at all. The results also show that task-related roll motion increases performance.

Participants were able to use the perceived roll motion to improve their precision in hovering in front of a target. This is an important result, because it shows for the first time that the unique feature of teleoperation, the spatial decoupling, can be exploited for the benefit of operating performance. This introduces the possibility of mitigating some of the negative effects that are introduced by the separation between operator and vehicle in teleoperation. In addition, it introduces the possibility of providing optimal motion feedback depending on the vehicle used and the task at hand.

However, the results have been found using a virtual quadrotor flying in a simulated environment. Proving the feasability of the approach in a real teleoperation setup was the goal of the experiment shown in chapter 4. In addition a general method of describing task-related motion feedback was introduced.

Chapter 4 describes the implementation of a teleoepration setup that allowed an operator to control a remote octorotor from within the motion simulator cabin over an extended time period. The teleoperation system was robust enough to be used in a teleoperation experiment. The experiment was a reproduction of the experiment described in chapter 3 with the same task and experimental conditions.

Although the results do not show significant differences between conditions, i.e., motion feedback did not significantly affect performance, we could find indications that participants used the motion feedback when controlling the octorotor. This shows the feasibility of implementing motion feedback in a teleoperations setup for the control of UAVs. Furthermore, the motion feedback definition introduced in Chapter 4 allowed to describe motion feedback by defining a single motion feedback transformation matrix M. Essentially, M allows to describe any linear combination of vehicle state and desired task state. This method uses the freedom granted by the spatial decoupling between operator and vehicle, enabling us to shape motion feedback to include task information.

The final study of this thesis found in chapter 5 focused on three research questions. Can task-related motion feedback increase performance in a collision avoidance task? Does vehicle state-related

motion feedback affect performance in the absence of external disturbances? A common approach for collision avoidance tasks in teleoperation is providing haptic feedback about obstacles. How does task-related motion feedback compare to haptic feedback?

In the experiment described in chapter 5 we measured performance by counting the number of collisions and completion time. In addition we described behavioral changes using the onset time of avoiding the obstacle, the distance to the obstacle while passing, and stick deflection.

Haptic and motion feedback are not mutually exclusive and can be presented simultaneously. A future experiment could investigate how providing both types of feedback simultaneously affects operator performance in teleoperation. In this future experiment the information contained in the feedback would differ to avoid redundancy. Haptic feedback could provide information about obstacles in the environment, while task-related motion feedback could provide feedback about a secondary task, e.g., tracking a predefined trajectory. This could enable operators to better control remote vehicles without the need for additional visual displays. In fact, a setup like this could potentially allow for operators to complete the task even in extremely poor visual conditions.

Bibliography

Alaimo, S. M. C., Pollini, L., Bresciani, J. P., and Bülthoff, H. H., "A comparison of direct and indirect haptic aiding for remotely piloted vehicles," *19th IEEE International Symposium on Robot and Human Interactive Communication*, pp. 541–547, September 2010.

Apostolos, M., Zak, H., Das, H., and Schenker, P., "Multisensory feedback in advanced teleoperations: benefits of auditory cues," vol. 1828, pp. 98–105, 1992.

Bach-y-Rita, P. and Kercel, S., "Sensory substitution and the human–machine interface," *Trends in cognitive sciences*, vol. 7, no. 12, pp. 541–546, 2003.

Bejczy, A., "Sensors, controls, and man-machine interface for advanced teleoperation," *Science*, vol. 208, no. 4450, pp. 1327–1335, June 1980.

Bouabdallah, S., Murrieri, P., and Siegwart, R., "Design and control of an indoor micro quadrotor," *Proceedings of the 2004 IEEE International Conference on Robotics and Automation*, vol. 5, pp. 4393–4398, April 2004.

Breen, B., "Controlled flight into terrain and the enhanced ground proximity warning system," *IEEE Aerospace and Electronic Systems Magazine*, vol. 14, no. 1, pp. 19–24, Jan 1999.

Brye, R., Frederick, P., Kirkpatrick III, M., and Shields Jr, N., "Earth orbital teleoperator manipulator system evaluation program," 1977.

Chen, J. Y. C., Haas, E. C., and Barnes, M. J., "Human performance issues and user interface design for teleoperated robots," *IEEE*

Transactions on Systems, Man, and Cybernetics, Part C: Applications and Reviews, vol. 37, no. 6, pp. 1231–1245, November 2007.

Cole, R. and Kishimoto, B., "Remote operator performance using bandwidth-limited tv displays: A review and proposal." Tech. rep., DTIC Document, August 1980.

Crooks, W., Freedman, L., and Coan, P., "Television systems for remote manipulation," *Proceedings of the Human Factors and Ergonomics Society Annual Meeting*, vol. 19, pp. 428–435, SAGE Publications, 1975.

Cui, J., Tosunoglu, S., Roberts, R., Moore, C., and Repperger, D., "A review of teleoperation system control," *Proceedings of the Florida conference on recent advances in robotics (FCRAR)*, 2003, florida Atlantic University, FL.

Giordano, P., Masone, C., Tesch, J., Breidt, M., Pollini, L., and Bülthoff, H., "A novel framework for closed-loop robotic motion simulation-part i: Inverse kinematics design," *IEEE International Conference on Robotics and Automation (ICRA)*, pp. 3876–3883, IEEE, 2010a.

Giordano, P., Masone, C., Tesch, J., Breidt, M., Pollini, L., and Bülthoff, H., "A novel framework for closed-loop robotic motion simulation-part ii: Motion cueing design and experimental validation," *IEEE International Conference on Robotics and Automation (ICRA)*, pp. 3896–3903, IEEE, 2010b.

Grabe, V., Riedel, M., Bülthoff, H., Giordano, P., and Franchi, A., "The TeleKyb framework for a modular and extendible ROS-based quadrotor control," *Proceedings of 6th European Conference on Mobile Robots (ECMR 2013)*, pp. 19–25, September 2013.

Griffiths, P. and Gillespie, R., "Sharing control between humans and automation using haptic interface: primary and secondary task performance benefits," *Human Factors: The Journal of the Human Factors and Ergonomics Society*, vol. 47, no. 3, pp. 574–590, 2005.

Hall, J., "The need for platform motion in modern piloted flight training simulators," Tech. rep., DTIC Document, October 1989.

Heinlein, R., *Waldo*, Doubleday, 1942.

Hing, J. T. and Oh, P. Y., "Development of an unmanned aerial vehicle piloting system with integrated motion cueing for training and pilot evaluation," Valavanis, K. P., Oh, P., and Piegl, L. A. (editors), *Unmanned Aircraft Systems*, pp. 3–19, 2009.

Hosman, R., *Pilot's Perception and Control of Aircraft Motions*, Ph.D. thesis, Delft University of Technology, 1996.

Hua, M., Hamel, T., Morin, P., and Samson, C., "A control approach for thrust-propelled underactuated vehicles and its application to vtol drones," *IEEE Transactions on Automatic Control*, vol. 54, no. 8, pp. 1837–1853, August 2009.

Lächele, J., Franchi, A., Bülthoff, H., and Giordano, P., "Swarmsimx: Real-time simulation environment for multi-robot systems," *Simulation, modeling, and programming for autonomous robots*, pp. 375–387, Springer, 2012.

Lächele, J., Pretto, P., Venrooij, J., and Bülthoff, H., "Motion feedback improves performance in teleoperating UAVs," *AHS International 70th Annual Forum*, Montreal, QC, Canada, May 2014.

Lächele, J., Pretto, P., Venrooij, J., and Bülthoff, H., "Effects of vehicle- and task-related motion feedback on operator performance in teleoperation," *AHS International 72th Annual Forum*, May 2016, to be published.

Lam, T., Mulder, M., and van Paassen, M., "Haptic interface for uav collision avoidance," *The International Journal of Aviation Psychology*, vol. 17, pp. 167–195, 2007.

Lam, T. M., Boschloo, H. W., Mulder, M., and van Paassen, M. M., "Artificial force field for haptic feedback in UAV teleoperation," *IEEE Transactions on Systems, Man, and Cybernetics, Part A*, vol. 39, no. 6, pp. 1316–1330, November 2009.

Lane, J., Carignan, C., Sullivan, B., Akin, D., Hunt, T., and Cohen, R., "Effects of time delay on telerobotic control of neutral buoyancy vehicles," *IEEE International Conference on Robotics and Automation, ICRA.*, vol. 3, pp. 2874–2879, IEEE, 2002.

Lokki, T. and Gröhn, M., "Navigation with auditory cues in a virtual environment," *IEEE MultiMedia*, vol. 12, no. 2, pp. 80–86, April 2005.

Loomis, J., Klatzky, R., Golledge, R., Cicinelli, J., James W. Pellegrino, and Fry, P., "Nonvisual navigation by blind and sighted: Assessment of path integration ability," *Journal of Experimental Psychology: General*, vol. 122, no. 1, pp. 73–91, May 1993.

Masone, C., Robuffo Giordano, P., and Bülthoff, H. H., "Mechanical design and control of the new 7-dof cybermotion simulator," pp. 4935–4942, IEEE, Piscataway, NJ, USA, May 2011.

Monen, J. and Brenner, E., "Detecting changes in one's own velocity from the optic flow," *Perception*, vol. 23, pp. 681–690, 1994.

Nagel, S., Carl, C., Kringe, T., Märtin, R., and König, P., "Beyond sensory substitution–learning the sixth sense," *Journal of neural engineering*, vol. 2, no. 4, pp. R13–R26, 2005.

Nieuwenhuizen, F. M. and Bülthoff, H. H., "The mpi cybermotion simulator: A novel research platform to investigate human control behavior," *Journal of Computing Science and Engineering*, vol. 7, no. 2, pp. 122–131, 2013.

Nieuwenhuizen, F. M., Mulder, M., van Paassen, M. M., and Bülthoff, H., "The influence of motion system characteristics on pilot control behaviour," pp. 204–218, Red Hook, NY, USA, 8 2011.

Oman, C., "Motion sickness: a synthesis and evaluation of the sensory conflict theory," *Canadian Journal of Physiology and Pharmacology*, vol. 68, no. 2, pp. 294–303, 1990.

Ortiz, J., Tapia, C., Rossi, L., Fontaine, J.-G., and Maza, M., "Description and tests of a multisensorial driving interface for vehicle

teleoperation," *Proceedings of the 11th International IEEE Conference on Intelligent Transportation Systems*, pp. 616–621, October 2008.

Pérez Yuste, A., "Early developments of wireless remote control: the telekino of torres quevedo," *Proceedings of the IEEE*, vol. 96, no. 1, pp. 186–190, 2008.

Petzold, B., Zaeh, M., Faerber, B., Deml, B., Egermeier, H., Schilp, J., and Clarke, S., "A study on visual, auditory, and haptic feedback for assembly tasks," *Presence: teleoperators and virtual environments*, vol. 13, no. 1, pp. 16–21, Feb 2004.

Pool, D. M., Mulder, M., van Paassen, M. M., and Van der Vaart, J. C., "Effects of peripheral visual and physical motion cues in roll-axis tracking tasks," *Journal of Guidance, Control, and Dynamics*, vol. 31, no. 6, pp. 1608–1622, November–December 2008.

Posner, M., Nissen, M., and Klein, R., "Visual dominance: an information-processing account of its origins and significance," *Psychological review*, vol. 83, no. 2, p. 157, 1976.

Pretto, P., Bresciani, J., Rainer, G., and Bülthoff, H., "Foggy perception slows us down," *eLife*, October 2012.

Quigley, M., Conley, K., Gerkey, B., Faust, J., Foote, T., Leibs, J., Wheeler, R., and Ng, A., "ROS: an open-source Robot Operating System," *ICRA Workshop on Open Source Software*, 2009.

Ranadive, V., "Video resolution, frame rate and grayscale tradeoffs under limited bandwidth for undersea teleoperation." Tech. rep., DTIC Document, March 1980.

Ricard, G. L. and Parrish, R. V., "Pilot differences and motion cuing effects on simulated helicopter hover," *Human Factors: The Journal of the Human Factors and Ergonomics Society*, vol. 26, no. 3, pp. 249–256, June 1984.

Robuffo Giordano, P., Deusch, H., Lächele, J., and Bülthoff, H. H., "Visual-vestibular feedback for enhanced situational awareness in teleoperation of uavs," *AHS International 66th Annual Forum*, pp. 2809–2818, AHS International, May 2010.

Ruff, H., Draper, M., Lu, L., Poole, M., and Repperger, D., "Haptic feedback as a supplemental method of alerting UAV operators to the onset of turbulence," *Proceedings of the Human Factors and Ergonomics Society Annual Meeting*, vol. 44, pp. 41–44, 2000.

Ruijgrok, G., *Elements of airplane performance*, Delft University Press, 2nd edn., 1996.

Scanlon, C. H., "Effect of motion cues during complex curved approach and landing tasks," Nasa technical paper, Arkansas State University, December 1987.

Sheridan, T., "Telerobotics," *Automatica*, vol. 25, no. 4, pp. 487–507, 1989.

Sheridan, T. and Ferrell, W., "Remote manipulative control with transmission delay," *IEEE Transactions on Human Factors in Electronics*, vol. 4, no. 1, pp. 25–29, 1963.

Steele, M. and Gillespie, R., "Shared control between human and machine: Using a haptic steering wheel to aid in land vehicle guidance," *Proceedings of the human factors and ergonomics society annual meeting*, vol. 45, pp. 1671–1675, 2001.

Tesla, N., "Method of and apparatus for controlling mechanism of moving vessels or vehicles," Nov. 1898, uS Patent 613,809.

Tvaryanas, A., "Visual scan patterns during simulated control of an uninhabited aerial vehicle (uav)," *Aviation, space, and environmental medicine*, vol. 75, no. 6, pp. 531–538, 2004.

van Erp, J., "Controlling unmanned vehicles: The human factors solution," *Advances in vehicle systems concepts and integration: RTO Meeting Proceedings*, vol. 44, 2000.

Venrooij, J., Mulder, M., Abbink, D., Van Paassen, M., van der Helm, F., and Bülthoff, H., "Admittance-adaptive model-based cancellation of biodynamic feedthrough," *IEEE International Conference on Systems, Man and Cybernetics (SMC)*, pp. 1946–1951, IEEE, 2014.

Williams, K., "A summary of unmanned aircraft accident/incident data: Human factors implications," Tech. rep., Civil Aerospace Medical Institute, Oklahoma City, OK 73125, December 2004.

Wu, B., Klatzky, R., Lee, R., Shivaprabhu, V., Galeotti, J., Siegel, M., Schuman, J., Hollis, R., and Stetten, G., "Psychophysical evaluation of haptic perception under augmentation by a handheld device," *Human Factors: The Journal of the Human Factors and Ergonomics Society*, vol. 57, no. 3, pp. 523–537, May 2015.

Zaal, P., Nieuwenhuizen, F., Mulder, M., and van Paassen, M., "Perception of visual and motion cues during control of self-motion in optic flow environments," *AIAA Modeling and Simulation Technologies Conference*, August 2006.

Zaal, P. M. T., Pool, D. M., de Bruin, J., Mulder, M., and van Paassen, M. M., "Use of pitch and heave motion cues in a pitch control task," *Journal of Guidance, Control, and Dynamics*, vol. 32, no. 2, pp. 366–377, March–April 2009.

Anhang A
Selbständigkeitserklärung

Ich, Johannes Lächele , erkläre hiermit, dass ich die zur Promotion eingereichte Arbeit mit dem Titel Motion feedback in the teleoperation of Unmanned Aerial Vehicles selbständig verfasst (soweit nicht anderweitig durch den Verweis auf zugrunde liegende Veröffentlichungen gekennzeichnet), nur die angegebenen Quellen und Hilfsmittel benutzt und wörtlich oder inhaltlich übernommene Stellen als solche gekennzeichnet habe. Ich erkläre, dass die Richtlinien zur Sicherung guter wissenschaftlicher Praxis der Universität Tübingen (Beschluss des Senats vom 25.5.2000) beachtet wurden.

Teile dieser Arbeit wurden in der vorliegenden Form im Zuge wissenschaftlicher Publikationen veröffentlicht und enthalten zu einem gewissen Anteil Überlegungen, Formulierungen und Ergebnisse der entsprechend ausgewiesenen Ko-Autoren. Die zugrunde liegenden Publikationen mit einer Auflistung der beteiligten Autoren sind in den jeweiligen Kapitelübersichten zitiert. Kleinere Beiträge weiterer Personen sind zudem in den entsprechenden Acknowledgments aufgeführt.

Ich versichere an Eides statt, dass diese Angaben wahr sind und dass ich nichts verschwiegen habe. Mir ist bekannt, dass die falsche Abgabe einer Versicherung an Eides statt mit Freiheitsstrafe bis zu drei Jahren oder mit Geldstrafe bestraft wird. Diese Promotionsarbeit wurde in gleicher oder ähnlicher Form in keinem anderen Studiengang als Prüfungsleistung vorgelegt.

Ort, Datum

Johannes Lächele